

# Structure–Activity Relationship Studies and Discovery of a Potent Transient Receptor Potential Vanilloid (TRPV1) Antagonist 4-[3-Chloro-5-[(1*S*)-1,2-dihydroxyethyl]-2-pyridyl]-*N*-[5-(trifluoromethyl)-2-pyridyl]-3,6-dihydro-2*H*-pyridine-1-carboxamide (V116517) as a Clinical Candidate for Pain Management

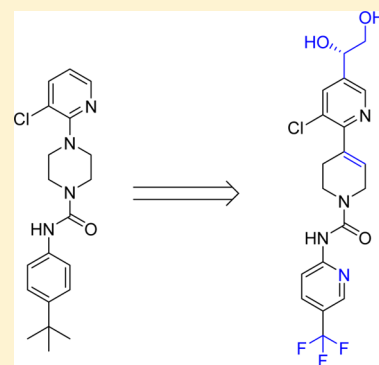
Laykea Tafesse,<sup>\*,†</sup> Toshiyuki Kanemasa,<sup>‡</sup> Noriyuki Kurose,<sup>‡</sup> Jianming Yu,<sup>†</sup> Toshiyuki Asaki,<sup>‡</sup> Gang Wu,<sup>†</sup> Yuka Iwamoto,<sup>‡</sup> Yoshitaka Yamaguchi,<sup>‡</sup> Chiyou Ni,<sup>†</sup> John Engel,<sup>†</sup> Naoki Tsuno,<sup>‡</sup> Aniket Patel,<sup>†</sup> Xiaoming Zhou,<sup>†</sup> Takuya Shintani,<sup>‡</sup> Kevin Brown,<sup>†</sup> Tsuyoshi Hasegawa,<sup>‡</sup> Manjunath Shet,<sup>†</sup> Yasuyoshi Iso,<sup>‡</sup> Akira Kato,<sup>‡</sup> and Donald J. Kyle<sup>†</sup>

<sup>†</sup>Discovery Research, Purdue Pharma LP, 6 Cedar Brook Drive, Cranbury, New Jersey 08512, United States

<sup>‡</sup>Shionogi Research Laboratories, Shionogi & Co., Ltd., 3-1-1 Futaba-chow, Toyonaka, Osaka, Japan

## **S** Supporting Information

**ABSTRACT:** A series of novel tetrahydropyridinecarboxamide TRPV1 antagonists were prepared and evaluated in an effort to optimize properties of previously described lead compounds from piperazinecarboxamide series. The compounds were evaluated for their ability to block capsaicin and acid-induced calcium influx in CHO cells expressing human TRPV1. The most potent of these TRPV1 antagonists were further characterized in pharmacokinetic, efficacy, and body temperature studies. On the basis of its pharmacokinetic, in vivo efficacy, safety, and toxicological properties, compound 37 was selected for further evaluation in human clinical trials.



## ■ INTRODUCTION

Capsaicin, the active ingredient of chili peppers, has been known for decades to specifically activate mammalian nociceptors and cause pain.<sup>1</sup> The cloning of the capsaicin receptor, TRPV1, transient receptor potential cation channel, subfamily V, member 1, by Julius and co-workers in 1997 has stimulated basic research on the transduction of noxious stimuli by sensory neurons at the molecular level and has facilitated the identification of novel drugs to treat pain by targeting this channel.<sup>2–5</sup> TRPV1 is a nonselective cation channel that is polymodal, being activated by multiple unrelated stimuli such as capsaicin, heat, low pH, and certain endogenous substances produced by inflamed tissues. Furthermore, TRPV1 is highly expressed by nociceptive sensory neurons. The expression is up-regulated in the presence of persistent inflammation. A critical role of TRPV1 in the development of inflammatory pain is supported by genetic inhibition of the channel in animals. In particular, TRPV1 knockout mice are devoid of experimentally induced thermal hypersensitivity with a pro-inflammatory substance.<sup>6,7</sup> Taken together, those features make TRPV1 to be an attractive molecular target for treating pain, especially pain associated with inflammation. In addition to pain transduction, TRPV1 has also been shown to play a central

role in the initiation of neurogenic inflammatory responses and may be a target for the treatment of other disorders such as cough, urinary incontinence, irritable bowel syndrome, and pruritus.

Identification of TRPV1 antagonists has been the focus of drug discovery efforts over the past several years by a number of pharmaceutical companies. A number of compounds have reached clinical development, including 1,<sup>8</sup> 2,<sup>9</sup> and 3<sup>10</sup> (Figure 1). In a phase I clinical trial with 2, dose-limiting hyperthermia occurred at subtherapeutic doses during postoperative dental pain studies.<sup>9</sup> Compound 3 also induced hyperthermia in healthy humans, but the magnitude was lower than what was reported for 2.<sup>10,11</sup> It is worth pointing out that hyperthermia was not described as one of the adverse effects for compound 1.<sup>4,8</sup> An additional unwanted side effect during clinical use of TRPV1 antagonists is their effect in altering temperature sensation. Clinical candidate 3 was reported to impair thermal sensation by elevating skin and oral heat pain thresholds.<sup>10</sup> This has raised concerns about a potential risk of burn injury to the skin or mouth for people who, for instance, take a hot water

Received: May 28, 2014

Published: July 24, 2014

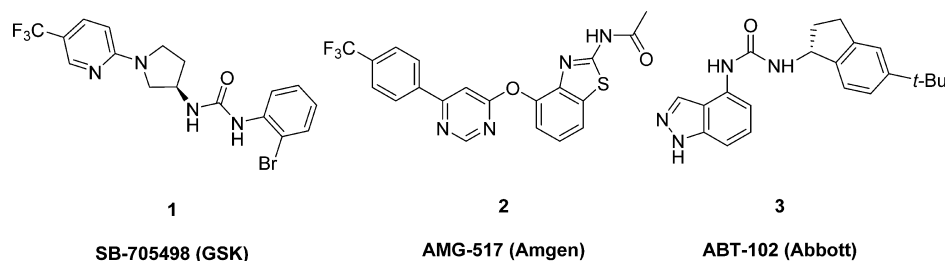


Figure 1. Structures of selected TRPV1 antagonists.

shower or drink hot coffee/tea. These unwanted side effects associated with the use of TRPV1 antagonists (i.e., hyperthermia and impairment of noxious thermal sensation) became the main dose-limiting factors in current clinical developments.<sup>3,5</sup> The underlying mechanisms behind these two unwanted side effects is unclear. In addition, the magnitude and duration of the side effects seems to be different for different molecules. Despite unclear mechanisms, pharmaceutical research to identify compounds with improved safety margin is underway by integrating body temperature and thermal sensation measurements in preclinical development strategy. The identification of novel TRPV1 antagonists with a wider safety margin will allow clinical trials designs to include higher dose groups for proof-of-concept studies that the field of TRPV1 research still awaits.

During the past decade, various structural classes of TRPV1 antagonists have been reported in the literature.<sup>12</sup> We previously described SAR study results of piperazinecarboxamides analogues such as **4** as potent TRPV1 antagonists.<sup>13</sup> Lead compounds from this series were highly potent and efficacious across a range of preclinical pain models. Despite this, development of lead compounds from this series was hindered due to a variety of issues including poor aqueous solubility and oral bioavailability. We, therefore, initiated our follow-up SAR effort with the aim of identifying novel potent TRPV1 antagonists with improved aqueous solubility, pharmacokinetic properties, and overall pharmaceutical profile. Our strategy to achieve this goal was based on a systematic exploration of polar, water solubilizing substitutions on pyridine ring A and aniline C. Our initial SAR exploration effort has led to the identification of tetrahydropyridine ring as a bioisosteric replacement for piperazine ring B (Figure 2). Therefore, in this article, we used tetrahydropyridine as the core ring B and describe SAR study results for rings A and C with emphasis on

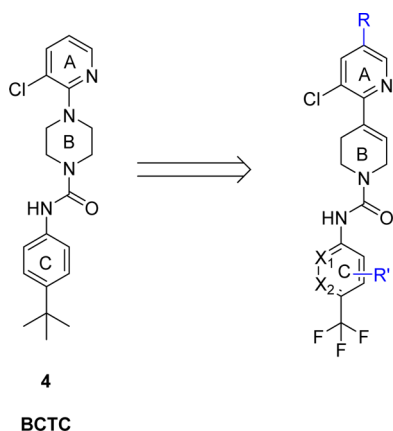


Figure 2. SAR approach based on piperazine carboxamides.

potency, aqueous solubility, and metabolic stability. This SAR study effort has culminated with the identification of compound **37**, a potent TRPV1 antagonist that is currently being evaluated in human clinical trials for treatment of pain.

## CHEMISTRY

The synthetic route employed to prepare analogues **9–16** is shown in Scheme 1. Commercially available *N*-Boc-1,2,3,6-tetrahydropyridine-4-boronic acid pinacol ester (**6**) was reacted with 2,4-dichloropyridine (**5**) by Suzuki coupling to give the corresponding *N*-Boc-tetrahydropyridine (**7**) in 79% yield. The Boc protecting group was removed by treatment with 4 N HCl in dichloromethane, leading to **8** as a hydrochloride salt in 95% yield. Intermediate **8** was then treated with different substituted and unsubstituted isocyanates in the presence of diisopropylethylamine (DIEA) as the base to give the corresponding targets (**9–16**) in good yields. Analogues (**20–29**) were prepared in a similar manner by using 5-substituted pyridines (**17a–j**) as starting materials instead of **5** (Scheme 2).

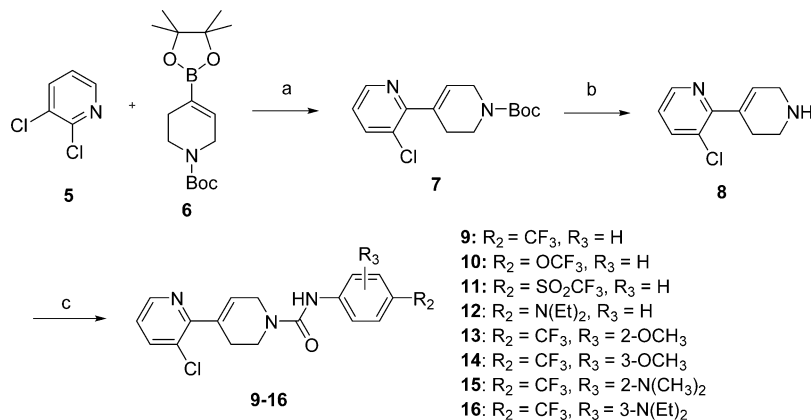
The synthesis of enantiomers (*S*)-**35** and (*R*)-**36** is outlined in Scheme 3. The 5-formyl group in 2,3-dichloro-5-formylpyridine (**30**) was converted to a vinyl group by reacting with methyltriphenylphosphonium bromide via Wittig reaction in the presence of *t*-BuOK in toluene to afford **31** in 70% yield. Subsequent asymmetric dihydroxylation of the vinyl group with either AD-mix- $\alpha$  or AD-mix- $\beta$  by using *t*-BuOH and water as co-solvents gave the corresponding (*S*)-diol **32a** (>95% ee) or (*R*)-diol **32b** (>95% ee) in 80% yield. Then Suzuki coupling of **32a** and **32b** with pinacole ester **6** afforded **33a** and **33b** in 80% yields. Deprotection of the boc protecting group with 4 N HCl followed by coupling with 4-(trifluoromethyl)phenyl isocyanate in the presence of diisopropylethylamine (DIEA) as the base gave analogues (*S*)-**35** and (*R*)-**36**.

The synthesis of analogues **37–39** is outlined in Scheme 4. Coupling reaction of **34a** with phenyl(5-(trifluoromethyl)pyridin-2-yl)carbamate or phenyl(6-(trifluoromethyl)pyridin-2-yl)carbamate in the presence of diisopropylethylamine (DIEA) in CH<sub>2</sub>Cl<sub>2</sub> afforded the corresponding ureas (*S*)-**37** and (*S*)-**38** in 74% and 70% yield, respectively. Similarly, coupling of **34b** with phenyl(5-(trifluoromethyl)pyridin-2-yl)carbamate gave (*R*)-**39** in good yield.

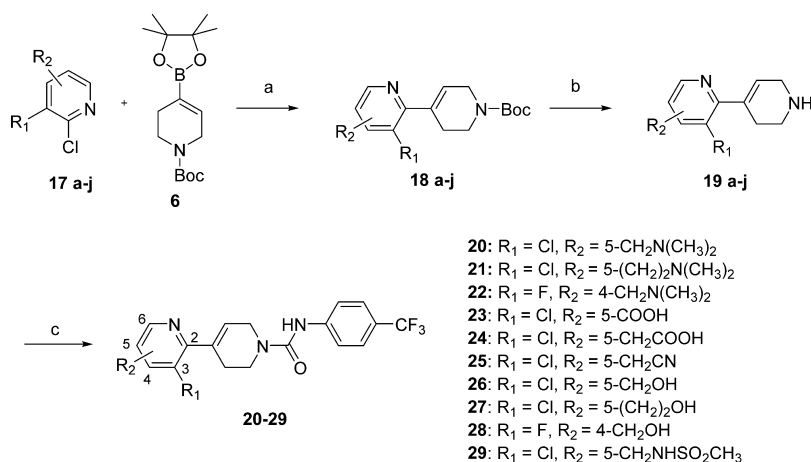
## RESULTS AND DISCUSSION

The compounds were evaluated for TRPV1 antagonist activity based on their ability to block capsaicin (CAP) or low pH-induced activation of human TRPV1 channel in CHO cell line. The tests were carried out in fluorescence-based calcium influx assays using FLIPR (Molecular Devices, CA) for CAP assay and FDSS (Hamamatsu Photonics, Japan) for pH assay.

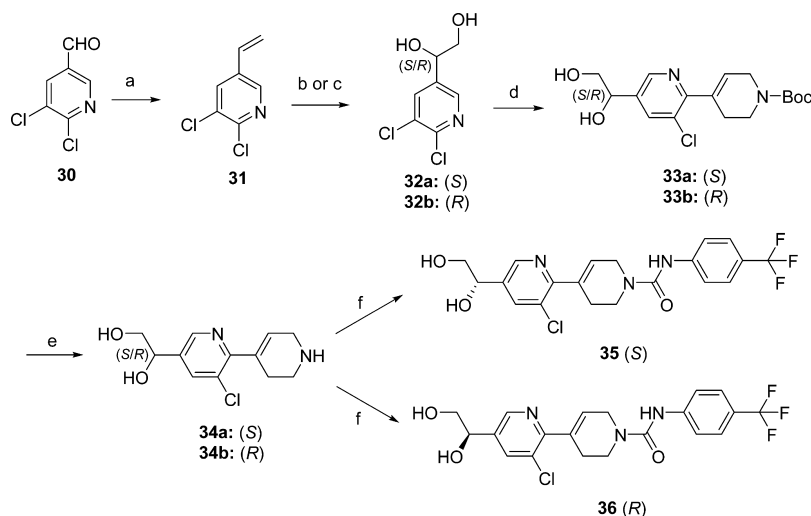
We began our investigation by replacing the piperazine ring of our previous lead molecules with tetrahydropyridine as a B-

Scheme 1. Synthesis of C-Ring Modified Tetrahydropyridine Analogues 9–16<sup>a</sup>

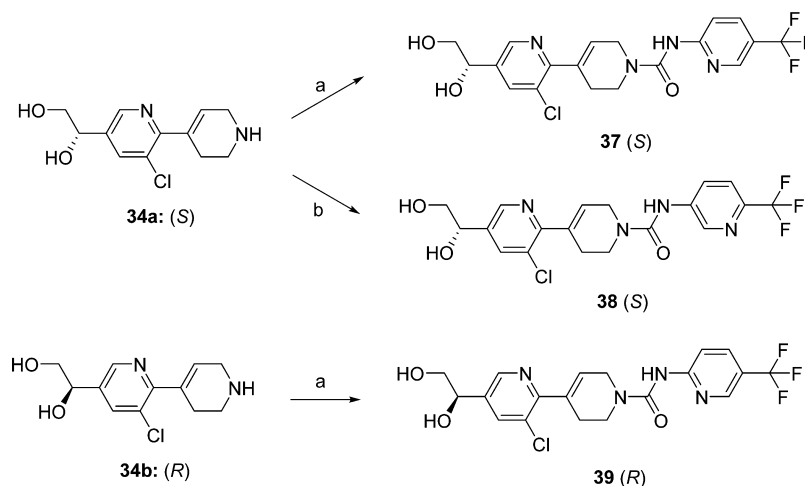
<sup>a</sup>Reagents and conditions: (a) Pd(PPh<sub>3</sub>)<sub>2</sub>Cl<sub>2</sub>, K<sub>2</sub>CO<sub>3</sub>, DME/EtOH/H<sub>2</sub>O (2:1:2), 90 °C; (b) 4 M HCl in Et<sub>2</sub>O, DCM, 45 °C; (c) substituted phenyl isocyanate or substituted *N*-phenyl-1*H*-imidazole-1-carboxamide, DIEA, DCM, 0 °C → rt.

Scheme 2. Synthesis of A-Ring Modified Analogues 20–29<sup>a</sup>

<sup>a</sup>Reagents and conditions: (a) Pd(PPh<sub>3</sub>)<sub>2</sub>Cl<sub>2</sub>, K<sub>2</sub>CO<sub>3</sub>, DME/EtOH/H<sub>2</sub>O (2:1:2), 90 °C; (b) 4 M HCl in Et<sub>2</sub>O, DCM, 45 °C; (c) 4-(trifluoromethyl)phenyl isocyanate, DIEA, DCM, 0 °C → rt.

Scheme 3. Synthesis of Dihydroxyl Analogues (*S*)-Diol 35 and (*R*)-Diol 36<sup>a</sup>

<sup>a</sup>Reagents and conditions: (a) PPh<sub>3</sub>CH<sub>3</sub>Br, *t*-BuOK, toluene; (b) AD-mix- $\alpha$ , *t*-BuOH/H<sub>2</sub>O (1:1), 0 °C → rt, then Na<sub>2</sub>SO<sub>3</sub>; (c) AD-mix- $\beta$ , *t*-BuOH/H<sub>2</sub>O (1:1), 0 °C → rt, then Na<sub>2</sub>SO<sub>3</sub>; (d) Pd(PPh<sub>3</sub>)<sub>2</sub>Cl<sub>2</sub>, K<sub>2</sub>CO<sub>3</sub>, 6, DME/EtOH/H<sub>2</sub>O (2:1:2), 90 °C; (e) 4 M HCl in Et<sub>2</sub>O, DCM, 45 °C; (f) 4-(trifluoromethyl)phenyl isocyanate, DIEA, DCM, 0 °C → rt.

Scheme 4. Synthesis of Pyridine Analogues 37–39<sup>a</sup>

<sup>a</sup>Reagents and conditions: (a) phenyl(5-(trifluoromethyl)pyridin-2-yl)carbamate, DIEA, DCM,  $-20\text{ }^{\circ}\text{C} \rightarrow \text{rt}$ ; (b) phenyl(5-(trifluoromethyl)pyridin-2-yl)carbamate, DIEA, DCM,  $0\text{ }^{\circ}\text{C} \rightarrow \text{rt}$ .

**Table 1. Effect of Aryl Group Modification on in Vitro Potency and ADME Properties**

no.	R <sub>1</sub>	R <sub>2</sub>	in vitro potency, IC <sub>50</sub> (nM) <sup>a</sup>		metabolic stability (% remaining)		solubility (μM)	
			CAP	pH	RLM	HLM	pH: 1.2	pH: 6.8
BCTC	<i>t</i> -Bu	H	2.9 ± 0.1	0.4 ± 0.1	0	19	24	0
<b>9</b>	CF <sub>3</sub>	H	135.9 ± 33.0	31.8 ( <i>n</i> : 1)	59	68	0	0
<b>10</b>	OCF <sub>3</sub>	H	211.2 ± 13.4	59.7 ± 5.9	57	106	>50	2
<b>11</b>	SO <sub>2</sub> CF <sub>3</sub>	H	103.7 ± 17.4	29.3 ± 4.8	62	103	>50	4
<b>12</b>	N(Et) <sub>2</sub>	H	469.4 ± 138.2		0	2	>50	40
<b>13</b>	CF <sub>3</sub>	2-OCH <sub>3</sub>	7633.8 ± 2690.5		47	73	>50	10
<b>14</b>	CF <sub>3</sub>	3-OCH <sub>3</sub>	156.6 ± 6.2	213.9 ± 31.7	37	17	>50	13
<b>15</b>	CF <sub>3</sub>	2-N(CH <sub>3</sub> ) <sub>2</sub>	>10000		15	29	>50	0.97
<b>16</b>	CF <sub>3</sub>	3-N(Et) <sub>2</sub>	124.2 ± 11.9	17.6 ± 3.4	0	0	>50	0.8

<sup>a</sup>IC<sub>50</sub> values are the mean ± SEM of at least three determinations unless otherwise stated.

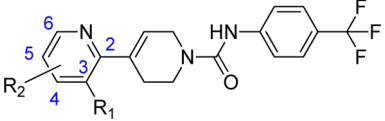
ring. This bioisosteric replacement was proven to be feasible as evidenced by favorable in vitro potency of compound **9**. Compound **9** was a good starting point for our lead optimization effort because of its favorable in vitro potency and metabolic stability. While the in vitro potency for compound **9** was acceptable, the compound showed very poor aqueous solubility and pharmacokinetic properties. In an effort to improve the aqueous solubility of such analogues, we initiated a detailed SAR study with the goal of introducing water solubilizing groups to pyridine ring-A and aniline ring-C.

We initially focused on the examining the effect of introducing polar substitutions on ring C (Table 1). Replacement of the lipophilic substitution CF<sub>3</sub> group at the 4-position of ring-C with OCF<sub>3</sub> or SO<sub>2</sub>CF<sub>3</sub>, as in compounds **10** and **11**, resulted in analogues that retained similar potency and metabolic stability to the lead compound **9**. Compounds **10** and **11** also showed significant improvements in aqueous solubility in acidic pH, however, their poor aqueous solubility in neutral pH made them less desirable for follow-up studies. A significant improvement in aqueous solubility was achieved

when the CF<sub>3</sub> group on ring-C of **9** was replaced with an amino group, as in **12**. The resulting analogue, however, showed a dramatic decrease in metabolic stability and a slight decrease in potency. Having explored few possible replacements for CF<sub>3</sub> group, we then focused our attention to study the influence of additional substitution on C-ring. We quickly learned that the position of the substitution on the aniline ring has a significant effect on potency. For example, while introduction of both amino and methoxy groups at 2-position of the ring-C, as in **13** and **15**, showed slight improvements in aqueous solubility, it resulted in a dramatic loss of potency. On the other hand, analogues with similar substitutions at 3-position of the aniline ring-C showed acceptable potency as demonstrated by compounds **14** and **16**. These 3-substituted analogues, however, did not provide good metabolic stability and aqueous solubility to justify advancement to additional studies.

We next examined the effect of introducing polar groups to ring-A of the lead compound **9** (Table 2). Most of the exploration was focused on the 5-position of the A-ring because that position was identified to be of tolerant of substitutions

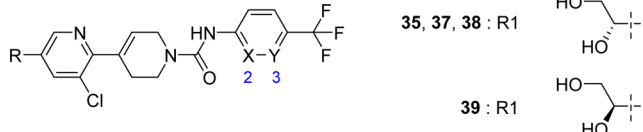
Table 2. Effect of Pyridine Ring Substitution on in Vitro Potency and ADME Properties



no.	R <sub>1</sub>	R <sub>2</sub>	in vitro potency, IC <sub>50</sub> (nM) <sup>a</sup>		metabolic stability (% remaining)		solubility (μM)	
			CAP	pH	RLM	HLM	pH: 1.2	pH: 6.8
9	Cl	H	135.9 ± 33.0	31.8 (n: 1)	59	68	0	0
20	Cl	5-CH <sub>2</sub> N(CH <sub>3</sub> ) <sub>2</sub>	923.5 ± 54.0		6	71	>50	>50
21	Cl	5-(CH <sub>2</sub> ) <sub>2</sub> N(CH <sub>3</sub> ) <sub>2</sub>	3166.7 ± 606.7		5	66	>50	>50
22	F	4-CH <sub>2</sub> N(CH <sub>3</sub> ) <sub>2</sub>	>25000		0	28	>50	>50
23	Cl	5-CO <sub>2</sub> H	>25000		95	96	29	>50
24	Cl	5-CH <sub>2</sub> CO <sub>2</sub> H	>25000		101	96	>50	>50
25	Cl	5-CH <sub>2</sub> CN	265.2 ± 69.0	165 (n: 1)	9	81	27	9
26	Cl	5-CH <sub>2</sub> OH	128.6 ± 26.0	41.7 ± 4.4	89	94	>50	>50
27	Cl	5-(CH <sub>2</sub> ) <sub>2</sub> OH	130.5 ± 20.0	185.3 ± 16.0	74	87	>50	10
28	F	4-CH <sub>2</sub> OH	7584.5 ± 1109.3		85	88	>50	24
29	Cl	5-CH <sub>2</sub> NHSO <sub>2</sub> CH <sub>3</sub>	471.3 ± 127.3		84	94	17	0.5
35	Cl	5-S-CH(OH)CH <sub>2</sub> OH	75.8 ± 12.4	11.6 ± 0.5	81	91	>50	>50
36	Cl	5-R-CH(OH)CH <sub>2</sub> OH	37.1 ± 14.8	38.3 ± 4.0	88	97	>50	>50

<sup>a</sup>IC<sub>50</sub> values are the mean ± SEM of at least three determinations unless otherwise stated.

Table 3. Effect of Switching Ring-C from Aniline to Pyridine



no.	X	Y	in vitro potency, IC <sub>50</sub> (nM) <sup>a</sup>		metabolic stability (% remaining)		solubility (μM)	
			CAP	pH	RLM	HLM	pH: 1.2	pH: 6.8
35	CH	CH	75.8 ± 12.4	11.6 ± 0.5	81	91	>50	>50
37	N	CH	35.1 ± 8.8	39.5 (n: 2)	85	97	>50	>50
38	CH	N	800.4 ± 63.3	5156.0 (n: 2)	94	102	>50	>50
39	N	CH	161.1 ± 41.7	223.3 ± 14.0	90	99	>50	>50

<sup>a</sup>IC<sub>50</sub> values are the mean ± SEM of at least three determinations unless otherwise stated.

based on previous SAR experience.<sup>13</sup> Introduction of basic center on ring-A for salt formation site, as in **20** and **21**, resulted in analogues that showed significant improvements on aqueous solubility in both acidic and neutral media. However, the in vitro potency as well as the metabolic stability of the resulting analogues was significantly reduced. We prepared compound **22** with the basic center moved to the 4-position of ring-A to explore the possibility of regaining in vitro potency. The resulting compound retained good aqueous solubility profile as expected, however, the substitution at this position was found to be detrimental for in vitro potency. We next explored the effect of introducing acidic groups at the 5-position of the A-ring. The introduction of acidic functionality to ring-A, as in **23** and **24**, offered much improved aqueous solubility and metabolic stability profile. However, the resulting compounds did not show potency at TRPV1. On the basis of these results, the possible use of acidic or basic functionality on ring-A was abandoned. We then prepared compound **25** to explore the effect of incorporating less polar substitutions on ring-A. Compound **25** showed about a 2-fold loss of potency in CAP assay and a 5-fold loss of potency in potency in pH assay. This result suggested that it may be possible to introduce a

substitution with some polarity at this position and still maintain potency. We next explored the use of small monohydroxyl groups such as methanol and ethanol, **26** and **27**, on ring-A. This modification resulted in significant improvements in aqueous solubility while also maintaining good in vitro potency and metabolic stability. The monohydroxyl compounds, **26** and **27**, showed very similar in vitro potencies when compared to compound **9** in CAP assay. In pH assay, the methanol substituted analogue **26** was about 4-fold more potent than the ethanol substituted analogue **27**. We also moved the hydroxyl group substitution to the 4-position on ring-A, compound **28**, and found that this was not tolerated for in vitro potency. We next explored the effect of introducing methylsulfonamide group, compound **29**, as a bioisosteric replacement for the hydroxyl group on compound **27**. This replacement did not seem to provide benefit, as the resulting compound showed about 4-fold less potency and also lower aqueous solubility neutral pH. Encouraged by the results from the monohydroxyl groups, we next explored the effect of introducing dihydroxyl group at the 5-position of ring-A, as in **35** and **36**. Both dihydroxyl substituted compounds showed excellent aqueous solubility and metabolic stability. In addition,

both compounds exhibited good in vitro potencies. The chirality of the dihydroxyl group did not seem to have an effect on the in vitro potency and metabolic stability of the initial two analogues.

Having identified an optimal substitution for pyridine ring-A that maintains good in vitro potency and metabolic stability, we then focused our attention on fine-tuning the ring-C (Table 3). It has previously been shown that the use of pyridine as a ring-C instead of aniline improves pharmaceutical properties of carboxamide analogues.<sup>14</sup> We, therefore, prepared dihydroxyl analogues using pyridine ring-C, as in 37, 38, and 39. All of the resulting analogues showed optimal metabolic stability and aqueous solubility profiles. Unlike the analogues 35 and 36 with an aniline ring-C, chirality of the dihydroxyl substitution on A-ring had a significant effect on the in vitro potency (e.g., 37 vs 39). The potency of *R*-enantiomer dihydroxyl compound 39 is about 5-fold less than its corresponding *S*-enantiomer compound 37 in both CAP and low pH assays. We have also found that the position of the pyridine nitrogen on ring-C pyridine nitrogen has significant effect on in vitro potency as shown by compounds 37 vs 38. Compound 37 with a pyridine nitrogen at 2-position is about 20-fold more potent in CAP assay and over 100-fold more potent in pH assay when compared to the compound with a pyridine nitrogen at 3-position, 38.

During our SAR investigation of this work, a reference describing the introduction of polar groups such as carboxylic acid and hydroxyl groups was published on a piperazine-benzimidazole class of TRPV1 antagonists.<sup>15</sup> In a similar manner to our findings, the reference described that hydroxyl groups on ring-A were well tolerated in the piperazine-benzimidazole series. The article described the synthesis and profile of a racemic dihydroxyl substitution in the piperazine-benzimidazole series. In our studies, we have found that the chirality of the dihydroxyl substitution can have significant effects on in vitro potency and pharmacokinetic properties of the resulting analogues. The article also describes that carboxylic acid substitutions are tolerated on pyridine ring-A in the piperazine-benzimidazole series. In our series of analogues, however, we have observed that the incorporation of a carboxylic acid at the 5-position of ring-A, as in 23 and 24, can be detrimental to in vitro potency.

Although the molecular structures of our compounds differ from capsaicin and other vanilloids, they are highly similar to our initial lead molecule 4, which was shown by Schild analysis to compete with capsaicin binding at the TRPV1 receptor.<sup>16</sup> On that basis, we propose that the mode of TRPV1 binding for our compounds is likely similar to 4 and thus interact significantly with key amino acid residues at or near the capsaicin binding site, although experimental proof of competitive binding remains to be obtained. Capsaicin is highly lipophilic and is presumed to penetrate the lipid bilayer then bind to the TRPV1 channel near the interface of the intracellular plasma membrane. Three important binding sites have been proposed for capsaicin binding to TRPV1 including two polar contacts (Arg114, Glu761) at the intracellular plasma membrane and a hydrophobic contact (described as the TM3 region) buried within the lipid bilayer domain of the channel.<sup>17,18</sup> Most TRPV1 antagonists, including our new compounds, contain three essential moieties in the pharmacophore, specifically a hydrogen bond donor, a hydrogen bond acceptor, and a ring. Recently published homology modeling of the TRPV1 channel–TRPV1 antagonist interaction proposes

that the hydrogen-bond acceptor moiety of the ligand may interact with Tyr 667 of the channel. The ring domain within the proposed antagonist pharmacophore fits within a hydrophobic space formed by the side chains of four Tyr 667 residues of the four monomers.<sup>17</sup>

Potent compounds, such as compound 26, 27, 35, 36, 37, and 39, that contain a substitution on A-ring, may conform to the known antagonist pharmacophore and therefore may interact comparably with other reported TRPV1 antagonists because they contain the hydrogen bond donor hydroxyl group, the hydrogen bond acceptor (trifluoromethyl), and the ring functionalities. We have not conducted specific homology modeling and docking simulations to evaluate this possibility directly, but we presume that such compounds would fit the proposed model given that it contains the three important pharmacophore elements of other known antagonists and given further a consideration of its overall molecular size, shape, and flexibility. Of interest in future molecular modeling studies would be an analysis of our surprising result showing that the diol-containing molecules block TRPV1 activation, while carboxylate- or amine-containing molecules do not. There are  $pK_a$  and steric differences between these functional groups that likely contribute to the explanation, but these differences may also reveal nuance in the character of the hydrogen bond donor functionality that is optimal for channel modulation.

The compounds that demonstrated acceptable in vitro potency, aqueous solubility, and metabolic stability were advanced into our preliminary pharmacokinetic screening studies (Table 4). Compounds 22, 26, 27, 35, 36, 37, and

**Table 4.** Rat Pharmacokinetic Parameters for Selected Compounds<sup>a</sup>

no.	$T_{1/2}$ (h) (iv)	CL (L/h/kg) (iv)	$V_d$ (L/kg)	$C_{max}$ (ng/mL) (po)	$F$ (%)
26	0.2	1.7	0.5	BQL	0
27	0.7	0.5	0.4	13	4
35	1.6	0.4	0.8	76	26
36	0.8	1.5	1.2	25	15
37	1.9	0.2	0.52	427	108
39	0.5	1.5	0.8	74	23

<sup>a</sup>Compounds dosed in DMA/PG (1:1) for iv (0.5 mg/kg), and 0.5% methylcellulose for po (1 mg/kg).

39 were dosed to rats intravenously (0.5 mg/kg) and orally (1 mg/kg). The monohydroxyl analogues 26 and 27 exhibited very short half-lives following intravenous administration and subsequently poor bioavailabilities after oral administration. The dihydroxyl analogues 35 and 36 showed higher systemic exposure after oral administration when compared to monohydroxyl analogues. It is interesting to note the effect the chirality of the dihydroxyl substitution has on the pharmacokinetic properties of the dihydroxyl analogues 35 and 36. The *S*-enantiomer analogue 35 demonstrated about 4-fold lower clearance after intravenous administration and 3-fold higher exposure after oral administration when compared to the *R*-enantiomer 36. This chirality effect on pharmacokinetic properties was consistent even when ring-C is switched to pyridine, e.g. 37 vs 39. The *S*-enantiomer dihydroxyl analogue 37 showed about 8-fold lower clearance after intravenous administration when compared to its corresponding *R*-enantiomer analogue 39. Compound 37 showed significantly improved plasma exposure ( $C_{max}$ : 427 ng/mL) and bioavail-

ability (108%) after oral administration, whereas the corresponding enantiomer, **39**, showed lower exposure ( $C_{\max}$ : 74 ng/mL) and bioavailability (23%) after oral administration. Because of its favorable in vitro potency, metabolic stability, and pharmacokinetic properties, compound **37** was selected as a lead candidate for pharmacokinetic, efficacy, and safety studies.

Compound **37** was screened for selectivity at 10  $\mu$ M in a panel of 66 ion channels, receptors, transporters, and enzymes (NovaScreen). Compound **37** had no interaction with any of the targets in the panel with the exception of a weak interaction with adenosine transporter (51.1%). In a follow-up experiment, the activity of compound **37** at adenosine transporter was determined to be 8.7  $\mu$ M. Selectivity of compound **37** versus other closely related TRP channels such as TRPV3 and TRPV4 was also evaluated. Compound **37** was highly selective for TRPV1 and did not show potency up to 10  $\mu$ M in both TRPV3 and TRPV4 assays (see Supporting Information).

A thorough examination of pharmacokinetic properties of compound **37** was conducted to determine its oral bioavailability and dose proportionality. As shown in Table 5,

**Table 5. Pharmacokinetic Parameters of Compound 37 after Single Oral Administration to Nonfasted Rats<sup>a</sup>**

pharmacokinetic parameters	dose			
	0.3 mg/kg	1 mg/kg	3 mg/kg	10 mg/kg
$C_{\max}$ (ng/mL)	131	447	1380	5630
$T_{\max}$ (h)	1.0	1.7	1.3	2.7
$AUC_{\text{inf}}$ ( $\mu$ g·h/mL) <sup>c</sup>	1.0	4.2	10.1	59.1
bioavailability (%) <sup>b</sup>	74	92	74	83

<sup>a</sup>Data are expressed as the mean of three rats. <sup>b</sup>Bioavailability (%) =  $\text{dose}(\text{iv})/\text{dose}(\text{po}) \times AUC_{\infty}(\text{po})/AUC_{\infty}(\text{iv}) \times 100$ . <sup>c</sup>Using  $AUC_{\text{iv}}$  1 mg/kg for BA of 0.3, 1, and 3 mg/kg, and using  $AUC_{\text{iv}}$  10 mg/kg for BA of 10 mg/kg.

bioavailability and plasma levels were high after oral administration of **37** at 0.3, 1, 3, and 10 mg/kg doses. For example, oral bioavailability of 1 mg/kg dose was 92% with  $C_{\max}$  of 447 ng/mL and the oral bioavailability of 3 mg/kg dose was 74% with  $C_{\max}$  of 1380 ng/mL. Dose-proportionality of compound **37** was also maintained between doses 0.3–3 mg/kg. Compound **37** showed low clearance and volume of distribution after intravenous administration at 1, 3, and 10 mg/kg (Table 6). In addition to plasma exposure studies, compound **37** was also evaluated for its ability to penetrate into CNS. The ratio of brain-to-plasma was assessed in rats at 3 h after oral administration of compound **37** at 3 mg/kg. The plasma concentration was 954 ng/mL and the brain concentration was 87 ng/mL. The ratio of brain-to-plasma

**Table 6. Pharmacokinetic Parameters of Compound 37 in Plasma after Single Intravenous Administration to Nonfasted Rats<sup>a</sup>**

pharmacokinetic parameters	dose		
	1 mg/kg	3 mg/kg	10 mg/kg
$AUC_{\text{inf}}$ ( $\mu$ g·h/mL)	4.6	14.4	71.6
$CL_{\text{tot}}$ (L/h/kg)	0.24	0.21	0.14
$t_{1/2}$ (h)	3.3	2.9	2.7
$V_{\text{dss}}$ (L/kg)	0.68	0.56	0.45

<sup>a</sup>Data are expressed as the mean of three rats.

concentration was determined to be 0.09, indicating that compound **37** is primarily restricted in periphery.

A comparative pharmacokinetic study was also conducted across preclinical species rat, dog, and monkey (Table 7).

**Table 7. Pharmacokinetic Parameters for Compound 37 after Intravenous (1 mg/kg) and Oral (3 mg/kg) Administration to Rats, Dogs, and Monkeys<sup>a</sup>**

species	$T_{1/2}$ (h) (iv)	CL (L/h/kg) (iv)	$V_d$ (L/kg)	$C_{\max}$ (ng/mL) (po)	F (%)
rat	3.3	0.24	0.68	1380	74
dog	3.6	0.28	1.2	1120	100
monkey	18	0.36	6.0	459	107

<sup>a</sup>Data are expressed as the mean of three animals.

Compound **37** showed very low clearance across species after intravenous administration at 1 mg/kg. After oral administration at 3 mg/kg, good plasma exposures were obtained in all three species. The oral bioavailabilities were 74% with a  $C_{\max}$  of 1380 ng/mL for rat, 100% with a  $C_{\max}$  of 1120 ng/mL for dog, and 107% with a  $C_{\max}$  of 459 ng/mL for monkey.

Prior to in vivo evaluations in rat pain models, we studied the ability of compound **37** to block the native TRPV1 channel in rat dorsal root ganglion (DRG) neurons. Whole cell patch clamp current recordings were performed to directly measure the channel activity. In this assay, compound **37** showed potent activity in inhibiting both CAP and low pH induced activation of native TRPV1 in a CAP-sensitive population of rat sensory neurons [ $IC_{50}$  = 423.2  $\pm$  39.1 nM ( $n$  = 3) for CAP;  $IC_{50}$  = 180.3  $\pm$  54.3 nM ( $n$  = 3) for acid] (Figure 3). Consistent with calcium influx data from recombinant TRPV1 (Table 2), this suggests that **37** belongs to the group of TRPV1 antagonists that block both CAP and low pH activations of TRPV1.<sup>19,20</sup> Furthermore, in the patch clamp assay it is apparent that the channel activity recovered quickly upon washout of the compound in both capsaicin and proton modes (Figure 4), suggesting that compound **37** has fast-off kinetics for antagonism of both mode activations of TRPV1.

In addition to in vitro electrophysiology (EP) study, we studied in vivo target engagement using capsaicin induced eye-wipe model in rats. In this model, compound **37** dose dependently reduced the number of eye-wipes induced by capsaicin. A significant reversal was demonstrated at 10 and 30 mg/kg oral doses for up to 5 h, proving that compound **37** has a long duration of action and that the in vivo efficacy is on target.

Compound **37** was then evaluated in acute inflammatory CFA model for its ability to reverse thermal hyperalgesia. In this model, compound **37** showed dose-dependent reversal of thermal hyperalgesia with an  $ED_{50}$  of 2 mg/kg (PO). The strong effect of compound **37** on inflammatory pain may be attributed to its high potency for blocking proton activation of TRPV1 in inflamed tissue (Figure 5). This supports the notion that the ability to block proton activation of TRPV1 is required for anti-inflammatory effects of TRPV1 antagonists.<sup>21</sup>

Several reports indicate that TRPV1 block is associated with an increase in core body temperature. We, therefore, evaluated the effects of compounds **37** on core body temperature after oral administration to rats implanted with telemetry devices (Figure 6). Similar to other previously described TRPV1 antagonist molecules, compound **37** caused dose-dependent increase in body temperature in rats after acute administration.

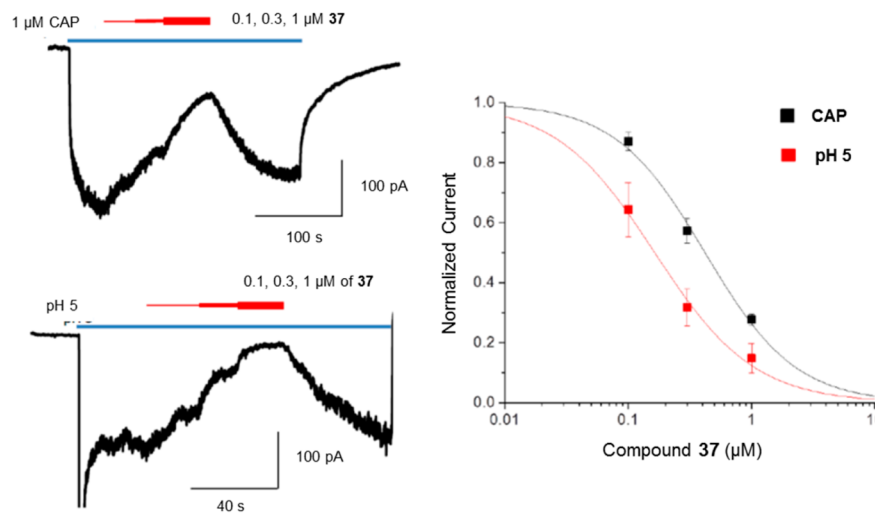


**Figure 3.** Inhibition by compound 37 of capsaicin (CAP)- and acid (pH 5)-induced currents in rat DRG neurons expressing native TRPV1. CAP (blue bar) induced inward currents in a population of rat DRG neurons, and the currents were inhibited by coapplication of compound 37 (red bar). Acid (pH 5, blue bar)-induced sustained inward currents were also inhibited by co-application of compound 37 (red bar) in a population of rat DRG neurons (responsive to CAP, not shown). Concentration–inhibition curves are plotted. Data are presented as the mean  $\pm$  SEM.

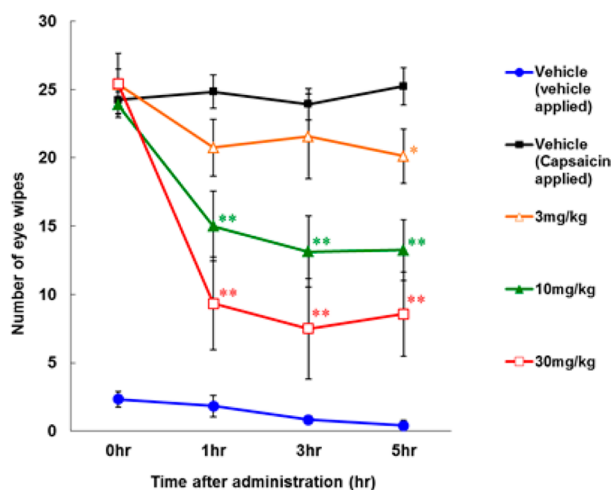


**Figure 4.** Effect of compound 37 in the eye-wipe test model after oral administration. Treatment with compound 37 dose dependently reduces the number of eye-wipes induced by capsaicin. Data are presented as the mean  $\pm$  SEM; (\*)  $p < 0.05$ , (\*\*)  $p < 0.01$  vs vehicle.

In this study, the maximum body temperature increase was capped at about 1.0 °C above vehicle controls even when 37 was dosed at exposures severalfold higher than analgesic doses. We also evaluated the effect of compound 37 on body temperature after repeated dosing. Compound 37 was dosed twice a day for 4 days, and rectal temperatures were measured by using a rectal probe thermistor. In agreement with previous reports, the increase in body temperature was attenuated after repeated administration of compound 37 (Table 8).

We next conducted body temperature and analgesic efficacy studies for 2 and compared its effects with compound 37. Compound 2 is withdrawn from clinical trials due to dose-limiting hyperthermia effects during postoperative dental pain studies. In our study, we found that compound 2 shows a large degree of separation between the dose–response curves for body temperature and analgesic efficacy (Figure 7). For compound 2, the dose–response curve for body temperature

study is left shifted compared to the dose–response curve for its analgesic efficacy. As a result, a significant increase in body temperature was observed for 2 even at subanalgesic doses. In contrast, compound 37 did not exhibit a leftward shift on the dose–response curve for its effects on body temperature when compared to its analgesic efficacy. It has previously been reported that the body temperature risk with TRPV1 block can only be minimized by designing compounds that show differential pharmacology, i.e., blocking CAP mode of activation and not pH.<sup>22</sup> However, in this case we have discovered a compound that blocks both CAP and pH modes of activation and yet shows a reduced risk for body temperature elevation when compared to comparator 2. The mechanism behind such differences in the magnitude of body temperature change is not yet clearly understood, however, it could be due to a combination of factors including receptor kinetics. Compound 37 showed fast off-rate in receptor kinetics study. This property of compound 37 is unique compared to previously reported clinical compounds such as 2 and 3, which exhibited slow-off rates. Additional details on our receptor kinetics study will be reported elsewhere.

A second undesirable clinical finding in the development of TRPV1 antagonist compounds was their effect of TRPV1 block on thermal sensitivity. In clinical studies using healthy subjects, compound 3 has previously been reported to cause impairment in thermosensation.<sup>10</sup> The effect was sustained over the dosing period, but recovery was fast after washout period. We used a hot plate test in order to assess the effect of compound 37 on thermal sensation in a preclinical setting.<sup>23</sup> The results from this study were compared with previous TRPV1 antagonist clinical compounds 2 and 3 (Figure 8). In our studies, we found that oral administration of all three compounds showed a dose-dependent reduction in thermal sensitivity. There was a very slight but favorable separation in dose–response curve between efficacy and temperature sensation for all three compounds. In this assay, compound 37 did not show any favorable advantage when compared to 2 or 3. A detailed analysis of the effect of compound 37 on thermosensation in a clinical setting will be the subject of future publication.

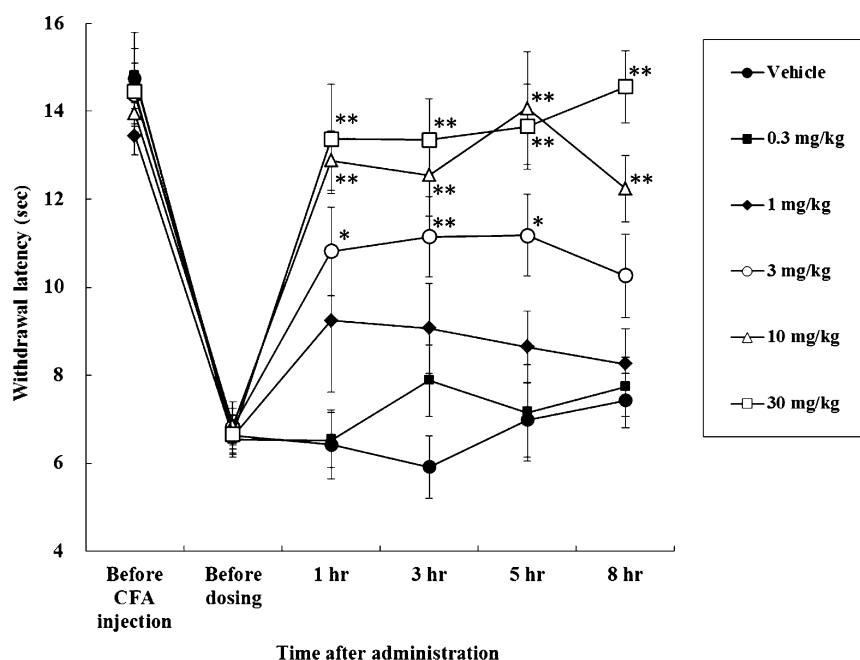


**Figure 5.** Efficacy of compound 37 in the CFA inflammatory pain model after oral administration to rats. Compound 37 dose-dependently reverses inflammatory thermal hyperalgesia. Data are presented as the mean  $\pm$  SEM; (\*)  $p < 0.05$ , (\*\*)  $p < 0.01$  vs vehicle.

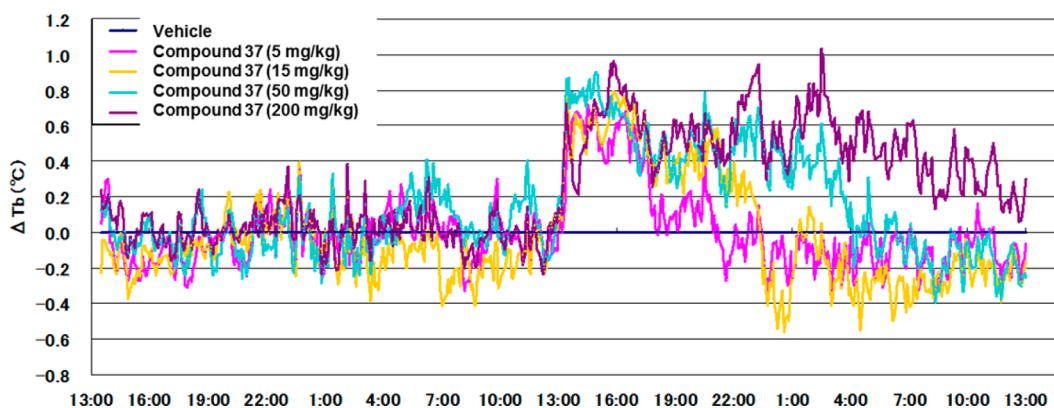


**Figure 6.** Body temperature changes as compared to vehicle following oral administration of compound 37 in rats. Compound 37 was administered at 13:00.

**Table 8. Maximal Body Temperature Changes As Compared to Vehicle Following Repeated Oral Administration of Compound 37 (10 mg/kg, bid) for 4 Days in Naïve Rats**

	day 1	day 2	day 3	day 4
$\Delta BT^a$	$0.95 \pm 0.20$	$0.71 \pm 0.16$	$0.64 \pm 0.11$	$0.41 \pm 0.12$

<sup>a</sup> $\Delta BT$  values are the mean  $\pm$  SEM of eight animals.

## SUMMARY

In conclusion, we have conducted SAR studies with the goal of identifying a novel development candidate with acceptable in vitro potency and overall pharmaceutical profile. This was achieved through systematic modifications of the different regions of the lead molecule: rings A, B, and C. The SAR study was initiated by replacing the piperazine ring portion of the lead molecules with a tetrahydropyridine ring. This was followed by detailed SAR with the goal of improving aqueous solubility, pharmacokinetic properties, and overall pharmaceutical profile of the lead compounds. This has led to the identification of the

S-enantiomer of a dihydroxyl substituent at the 5-position of A-ring as an optimal group for improving aqueous solubility and pharmacokinetic properties while maintaining excellent in vitro potency.

The development of TRPV1 antagonists have been hampered by dose-limiting side effects such as hyperthermia and effects on temperature sensation. To this end, we have demonstrated that analgesic efficacy can be separated from the unwanted side effects by profiling 37 alongside the clinical comparator 2 in preclinical studies. Although compound 37 does not show mode-selective antagonism of TRPV1 for capsaicin and proton, its pharmacology is unique in that it shows fast-off kinetics in EP assay using CAP and pH as stimulants when compared to 2. The results of this receptor kinetics study will be the subject of future publication.

In summary, compound 37 showed good in vitro potency, aqueous solubility, metabolic stability, oral bioavailability in multiple species, and excellent efficacy in a variety of animal pain models. After extensive safety and toxicology studies,

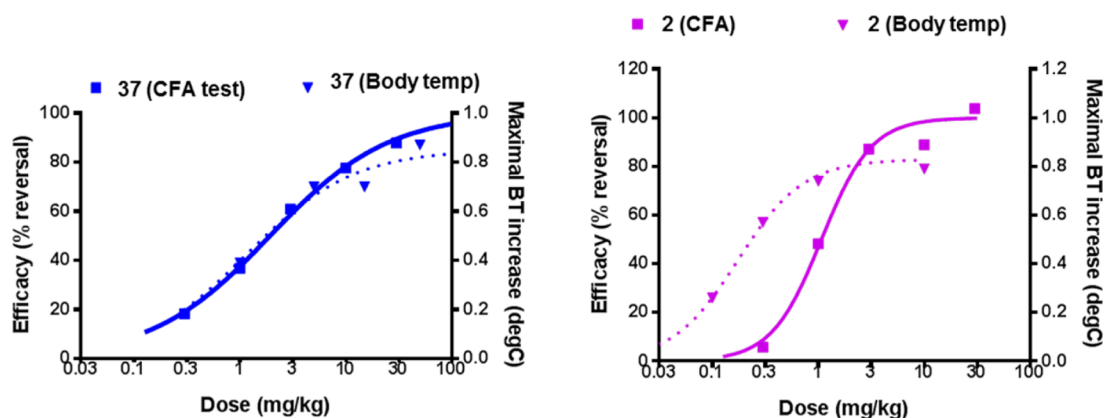


**Figure 7.** Plot comparing the effect of 37 or 2 on body temperature and pain in rats. Maximal body temperature changes (as compared to time-matched vehicle) and maximal percent reversal of CFA inflammatory pain are plotted against the oral dose.

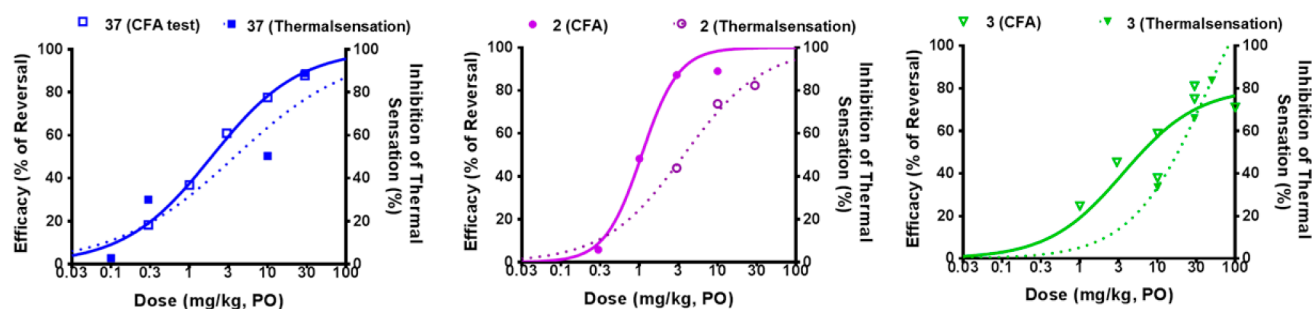


**Figure 8.** Plot comparing the effect of 37, 2, and 3 on pain and thermal sensation in rats. Maximal percent reversal of CFA inflammatory pain and maximal percent inhibition of thermal sensation in the hot plate test are plotted against oral dose.

compound 37, named as V116517, was selected to advance into clinical trials.

## EXPERIMENTAL SECTION

**TRPV1 Functional Assay.** Cell-based fluorescence assays of calcium influx upon TRPV1 activation were performed according to previous described methods with modifications.<sup>16,21</sup> In brief, CHO cells stably overexpressing the human TRPV1 (hTRPV1) channel (GenBank accession AJ277028) were cultured in DMEM supplemented with 2 mM L-glutamine and 10% fetal bovine serum in an incubator (5% CO<sub>2</sub>) at 37 °C.

For capsaicin activation assay, cells were seeded in 96-well plates 24 h before measurements of Ca<sup>2+</sup> influx were performed using Fluorescence Imaging Plate Reader (FLIPR; Molecular Devices). Plates were washed with Hank's Solution (Life Technologies) containing 1.6 mM CaCl<sub>2</sub> and 20 mM HEPES (pH 7.4) before loading of cells with Fluo-4 (3 μM × 1 h at 37 °C) in the presence of 2.5 mM probenecid. Cells were washed and then transferred to the FLIPR. After a 15 s baseline reading, cells were incubated with test compounds for 2 min before addition of the agonist (100 nM capsaicin), and fluorescence was read for additional 3 min.

In the pH assay, cells were seeded in 96-well plates for 2 or 3 days before measurements of Ca<sup>2+</sup> influx performed using FDSS-3000 (Hamamatsu Photonics, Japan). After washout of culture medium, cells were loaded with Fura-2 AM (5 μg/mL) and 0.5% Pluronic F127 in the loading buffer for 50–60 min at 37 °C. The loading buffer was composed of 20 mM HEPES, 115 mM NaCl, 5.4 mM KCl, 0.8 mM MgCl<sub>2</sub>, 1.8 mM CaCl<sub>2</sub>, 13.8 mM D-glucose, and 2.5 mM probenecid (pH 7.4). Cells were washed and incubated with test compounds in measuring buffer at 4 °C for 15–20 min before being transferred to the FDSS-3000. After a baseline collection, acid pH solution was added to cells to activate hTRPV1 (final pH 5.0–5.1 by titration with 1 N H<sub>2</sub>SO<sub>4</sub>). The measuring buffer was composed of 20 mM HEPES, 115 mM NaCl, 5.4 mM KCl, 0.8 mM MgCl<sub>2</sub>, 1.8 mM CaCl<sub>2</sub>, and 13.8

mM D-glucose (pH 7.4), supplemented with 0.1% BSA and 5 mM CaCl<sub>2</sub>.

**Sensory Neuron Assay.** Whole cell patch clamp recordings and primary culture of sensory neurons from dorsal root ganglia (DRGs) were conducted according to previously described methods.<sup>6,24</sup> In brief, DRG were harvested from postnatal (P2–P4) Sprague–Dawley rats. Following trypsinization (2.5%; Invitrogen, Carlsbad, CA) in Ham's F-12 media, the digested tissue was rinsed with F-12 media containing 10% fetal calf serum. The tissue was triturated and plated on PDL/laminin coated coverslips (BD Biosciences, San Jose, CA) in neurobasal media supplemented with B27 (Invitrogen, Carlsbad, CA) and 50 ng/mL 2.5S mouse NGF (Sigma, St. Louis, MO). The plated neurons were incubated at 37 °C in 5% CO<sub>2</sub> for up to 3 days during which whole-cell voltage-clamp recordings were made using an Axopatch 200B amplifier and the pClamp software (Axon Instruments Inc., Union City, CA) using conventional patch-clamp techniques at room temperature (22–24 °C). Currents were obtained at a hold potential of –70 mV with Borosilicate patch pipettes (resistance: 1.5–3 MΩ), low pass filtered at 2–5 kHz and digitized at 1 kHz. The external solution contained (mM): NaCl (145), KCl (5), CaCl<sub>2</sub> (2), MgCl<sub>2</sub> (1), glucose (10), HEPES (10), pH 7.3. The internal solution was (mM): KCl (140), CaCl<sub>2</sub> (1), MgCl<sub>2</sub> (2), EGTA (11), pH 7.4. For proton activation, HEPES was replaced with MES (2-(N-morpholino)ethanesulfonic acid, 4-morpholineethanesulfonic acid) in the external solution, and the solution was adjusted to pH 5 with HCl. Acidic pH, capsaicin, and test compounds were applied to cells using an array of glass pipettes together with the fast-switching solution exchange system (SF-77B; Warner Instruments, Hamden, CT).

**Eye-Wipe Test.** Male Sprague–Dawley rats (6 weeks, 180–280 g) were used. Eye-wiping behavior was measured before (0 h) and at 1, 3, and 5 h of after oral dosing with vehicle or the compounds. Rats were acclimated for 10–20 min in 10 × 20 × 15 cm<sup>3</sup> acrylic glass chambers (Neuroscience, Japan) before testing at each time point. Capsaicin solution (100 μM in 10% ethanol/PBS) or the eye solution vehicle (10% ethanol/PBS) was applied into one eye (3 μL/eye) with a pipet

at each time point. The number of forelimb eye-wiping movements during 2 min was counted immediately after application of capsaicin or the solution control. Bilateral eye wiping (moving both fore limbs simultaneously) and wiping of the opposite, untreated eye were not counted. Data from any animal that continued eye wiping with grooming for more than 2 min at each time point, or that showed 40 or greater eye wipes during 2 min were excluded because eye wiping in response to capsaicin-induced pain does not normally continue beyond 1 min.<sup>25</sup> Statistical analysis was performed by Windows SAS program. The statistical tests (*p* value) were performed at a 2-sided 0.05 level.

**CFA Efficacy Test.** Male Sprague–Dawley rats (6 weeks, 180–280 g) were used. Pharmacodynamic response was measured in terms of withdrawal latency to a thermal stimulus applied to the left hind paw using Plantar Test Instrument (Ugo-Basil, Italy). CFA (50  $\mu$ L of 50% FCA) was injected into the left hind paw. Withdrawal latency was measured just before FCA injection to provide a pre-CFA value. Approximately 22 h after the CFA injection, the withdrawal latency was measured before the compound administration, and 1, 3, 5, and 8 h after.

The efficacy data comprised the % of reversal value at 1, 3, 5, and 8 h after the compound administration calculated as follows; % of reversal = (withdrawal latency for the CFA-injected left paw at each time point after the compound administration – withdrawal latency for the CFA-injected left paw before the compound administration)/(withdrawal latency for the left paw before CFA injection – withdrawal latency for CFA-injected left paw before the compound administration)  $\times$  100. The 0.5 w/v% methylcellulose aqueous solution was prepared as vehicle. Statistical analysis was performed by Windows SAS program. The statistical tests (*p* value) were performed at a 2-sided 0.05 level.

**Body Temperature Test (Telemetry).** Male Sprague–Dawley rats (7 weeks, 180–280 g) were used. Transmitters (G2 E-Mitter, Philips Respironics) were implanted in the intra-abdominal cavity under anesthesia with isoflurane. After the surgery, the operation sites were disinfected with an antiseptic solution (Iodine solution 10%, Meiji Seika Pharma, Japan). Following a recovery period of 5–7 days, rats were used in the experiment after they were confirmed to be devoid of any abnormalities in their general condition (i.e., only healthy animals were used). The rats were treated for acclimation in a plastic cage (1 animal/cage) beginning several days before the compound administration. Mean body temperature (BT) for each 5 min recording was automatically recorded by a data computer system (Vital View, Philips Respironics) via telemetry signals from each animal. BT was continuously recorded from 24 h before to 24 h after the compound administration. Mean BT were calculated for each group at each time point. Differences from mean of the vehicle group ( $\Delta$ BT) were calculated at each time point. Each time point was representative of data averaged over 1 h. The 0.5 w/v% methylcellulose aqueous solution was prepared as vehicle.

**Body Temperature Test (Thermistor).** Male Sprague–Dawley rats (7 weeks, 180–280 g) were used. A digital probe thermistor (TD300, Shibaura Electronics, Japan) was used for this study. A day before the actual study period, rats were habituated to handling for rectal probe insertion and oral dosing procedures. On evaluation days (days 1 to 4), rectal body temperatures were measured at 9:00, 10:00, 10:30, 11:00, 12:00, 13:00, 14:00, 15:00, 16:00, 17:00, 17:30, and 18:00. Compound 37 (10 mg/kg) or vehicle was orally administered at 10:00 and 17:00 for 4 days. A 0.5 w/v% methylcellulose aqueous solution was used as vehicle. Mean BT were calculated for each group at each time point on each day. Differences from mean of the vehicle group ( $\Delta$ BT) were calculated at each time point on each day.

**Thermal Sensation Test.** Male Sprague–Dawley rats (6 weeks, 180–280 g) were used. Rats were placed on a hot plate heated to 50  $^{\circ}$ C, and the time interval to flinching of their hind paws (response latency) was recorded by stop watch. If no response was obtained within 30 s (designated as the “cutoff time”), the rats were removed from the hot plate to avoid tissue injury. Prior to the compound administration, the response latency was measured on a single occasion to familiarize the animals. The response latency was

measured once at 3 h after the compound administration. The % inhibition of thermal sensation was calculated as follows;  $100 \times (L_c - L_v)/(30 - L_v)$ , where  $L_c$  and  $L_v$  are average response latency in the compound and vehicle administered groups, respectively. The 0.5 w/v% methylcellulose aqueous solution was prepared as vehicle.

**Pharmacokinetic Studies.** Male Sprague–Dawley rats were used. The intravenous doses were formulated as *N,N*-dimethylacetamide (DMA)/propylene glycol (PG) = 1/1(v/v) solution while the oral doses 0.5% methyl cellulose suspension. Blood samples were collected from the cannula inserted into jugular vein using a syringe containing anticoagulant. Male beagle dogs and female cynomolgus monkeys were administered at doses of 1 mg/kg iv or 3 mg/kg po, formulated as DMA/PG/25% hydroxylpropyl- $\beta$ -cyclodextrin solution = 1/1/2 (v/v/v) solution for iv and as 0.5% methyl cellulose suspension for po. Blood samples were collected from the limb vein using a syringe containing anticoagulant. Their blood samples were centrifuged to obtain plasma for LC/MS/MS analysis. The pharmacokinetic parameters were calculated by WinNonlin (version 5.0.1, Pharsight Corporation) based on a noncompartment model with uniform weighting.

**Chemistry. General Information.** All reagents and solvents including anhydrous solvents were of commercial quality and used without further purification. All reactions were carried out under a static atmosphere of nitrogen or argon and stirred magnetically unless otherwise stated. All flash chromatographic separations were performed using ISCO RediSep disposable silica gel column eluting with EtOAc/hexanes or methanol/CH<sub>2</sub>Cl<sub>2</sub>. All final compounds were purified to >95% purity as determined by two LC/MS methods. <sup>1</sup>H NMR spectra were recorded on either Bruker 400 or 500 MHz. Chemical shifts are specified in ppm referenced to deuterated solvent peaks.

**tert-Butyl 3-Chloro-5',6'-dihydro-(2,4'-bipyridine)-1'(2'H)-carboxylate (7).** To a mixture of 5 (1.45 g, 10 mmol), pinacol ester 6 (3.09 g, 10 mmol), and potassium carbonate (2.07 g, 15 mmol) in DME/EtOH/H<sub>2</sub>O (2/1/2, 50 mL) at room temperature was added Pd(PPh<sub>3</sub>)<sub>2</sub>Cl<sub>2</sub> (702 mg, 1.0 mmol). The resulting reaction mixture was degassed and heated at 95  $^{\circ}$ C for 10 h. After this period, the reaction mixture was cooled, diluted with water, extracted with CH<sub>2</sub>Cl<sub>2</sub> (50 mL  $\times$  2), dried over Na<sub>2</sub>SO<sub>4</sub>, and concentrated under reduced pressure to provide a crude product as a yellow oil. The crude sample was chromatographed by silica gel column chromatography eluting with a gradient of 20–50% ethyl acetate in hexanes to provide 7 (2.32 g, 79% yield) as a pale-yellow oil. <sup>1</sup>H NMR (400 MHz, CDCl<sub>3</sub>)  $\delta$  8.53 (d, *J* = 4.5 Hz, 1H), 7.81 (d, *J* = 7.9 Hz, 1H), 7.24 (m, 1H), 6.18 (m, 1H), 4.15 (m, 2H), 3.69 (t, *J* = 5.3 Hz, 2H), 2.63 (m, 2H), 1.52 (s, 9H). MS *m/z* 317.2 [M + Na]<sup>+</sup>.

**3-Chloro-1',2',3',6'-tetrahydro-2,4'-bipyridine (8).** To a solution of 7 (0.90 g, 3.0 mmol) in CH<sub>2</sub>Cl<sub>2</sub> (10 mL) at 0  $^{\circ}$ C was added 4 M HCl in Et<sub>2</sub>O (10 mL). The ice bath was removed and the resulting mixture was stirred at 40  $^{\circ}$ C for 20 h. After this period, the reaction mixture was allowed to cool to room temperature and the resulting solid was filtered, washed with Et<sub>2</sub>O (20 mL), and dried under reduced pressure to provide 8 as an HCl salt (0.66 g, 95% yield) as a white solid. <sup>1</sup>H NMR (400 MHz, CD<sub>3</sub>OD)  $\delta$  8.40 (dd, *J* = 4.7, 1.3 Hz, 1H), 7.84 (dd, *J* = 8.2, 1.4 Hz, 1H), 7.27 (dd, *J* = 8.2, 4.7 Hz, 1H), 6.08 (m, 1H), 3.79 (m, 2H), 3.37 (t, *J* = 6.1 Hz, 2H), 2.71 (m, 2H). MS *m/z* 195 [M + H]<sup>+</sup>.

**3-Chloro-N-[4-(trifluoromethyl)phenyl]-3',6'-dihydro-(2,4'-bipyridine)-1'(2'H)-carboxamide (9).** To a suspension of 8 (199 mg, 0.86 mmol, HCl salt) in anhydrous CH<sub>2</sub>Cl<sub>2</sub> (10 mL) at 0  $^{\circ}$ C was added diisopropylethylamine (DIEA, 1 mL) and 1-isocyanato-4-(trifluoromethyl)benzene (161 mg, 0.86 mmol). The reaction mixture was warmed to room temperature and stirred for an additional 2 h. The resulting mixture was concentrated under reduced pressure, and the residue was chromatographed by silica gel column chromatography eluting with a gradient of 0–20% MeOH in CH<sub>2</sub>Cl<sub>2</sub> to provide 9 (306 mg, 80% yield) as a white solid. <sup>1</sup>H NMR (400 MHz, DMSO-*d*<sub>6</sub>)  $\delta$  8.98 (s, 1H), 8.53 (dd, *J* = 4.7, 1.4 Hz, 1H), 7.97 (dd, *J* = 8.1, 1.3 Hz, 1H), 7.73 (d, *J* = 7.5 Hz, 2H), 7.60 (d, *J* = 8.8 Hz, 2H), 7.36 (dd, *J* =

8.1, 4.6 Hz, 1H), 6.23 (m, 1H), 4.27–4.13 (m, 2H), 3.70 (t,  $J = 5.6$  Hz, 2H), 2.64–2.52 (m, 2H). MS  $m/z$  382.2  $[M + H]^+$ .

**3-Chloro-N-[4-(trifluoromethoxy)phenyl]-3',6'-dihydro-(2,4'-bipyridine)-1'(2'H)-carboxamide (10).**  $^1H$  NMR (400 MHz,  $CDCl_3$ )  $\delta$  8.50 (dd,  $J = 4.6, 1.5$  Hz, 1H), 7.73 (dd,  $J = 8.1, 1.5$  Hz, 1H), 7.46–7.38 (m, 2H), 7.22–7.13 (m, 3H), 6.40 (s, 1H), 6.20 (dt,  $J = 3.3, 1.7$  Hz, 1H), 4.23 (m, 2H), 3.77 (t,  $J = 5.6$  Hz, 2H), 2.77–2.68 (m, 2H). MS  $m/z$  398.1  $[M + H]^+$ .

**3-Chloro-N-[4-[(trifluoromethyl)sulfonyl]phenyl]-3',6'-dihydro-(2,4'-bipyridine)-1'(2'H)-carboxamide (11).**  $^1H$  NMR (400 MHz,  $CDCl_3$ )  $\delta$  8.50 (dd,  $J = 4.7, 1.4$  Hz, 1H), 7.95 (d,  $J = 9.0$  Hz, 2H), 7.80–7.61 (m, 3H), 7.20 (dd,  $J = 8.1, 4.6$  Hz, 1H), 6.80 (s, 1H), 6.21 (dt,  $J = 3.2, 1.7$  Hz, 1H), 4.27 (m, 2H), 3.80 (t,  $J = 5.7$  Hz, 2H), 2.80–2.69 (m, 2H). MS  $m/z$  446.1  $[M + H]^+$ .

**3-Chloro-N-[4-(diethylamino)phenyl]-3',6'-dihydro-(2,4'-bipyridine)-1'(2'H)-carboxamide (12).**  $^1H$  NMR (400 MHz,  $CD_3OD$ )  $\delta$  8.87–8.77 (m, 1H), 8.74–8.66 (m, 1H), 8.05–7.97 (m, 1H), 7.75 (d,  $J = 9.0$  Hz, 2H), 7.53 (d,  $J = 8.8$  Hz, 2H), 6.48 (s, 1H), 4.40 (s, 2H), 3.88 (t,  $J = 5.3$  Hz, 2H), 3.77–3.54 (m, 4H), 2.75 (s, 2H), 1.17 (t,  $J = 7.2$  Hz, 6H). MS  $m/z$  385.2  $[M + H]^+$ .

**3-Chloro-N-[2-methoxy-4-(trifluoromethyl)phenyl]-3',6'-dihydro-(2,4'-bipyridine)-1'(2'H)-carboxamide (13).**  $^1H$  NMR (400 MHz,  $CD_3OD$ )  $\delta$  8.82–8.71 (m, 1H), 8.68–8.56 (m, 1H), 8.01 (d,  $J = 9.0$  Hz, 1H), 7.97–7.56 (m, 1H), 7.29–7.22 (m, 2H), 6.43 (s, 1H), 4.38 (m, 2H), 3.99 (s, 3H), 3.85 (t,  $J = 5.5$  Hz, 2H), 2.73 (d,  $J = 2.0$  Hz, 2H). MS  $m/z$  412.2  $[M + H]^+$ .

**3-Chloro-N-[3-methoxy-4-(trifluoromethyl)phenyl]-3',6'-dihydro-(2,4'-bipyridine)-1'(2'H)-carboxamide (14).**  $^1H$  NMR (400 MHz,  $CD_3OD$ )  $\delta$  8.37 (dd,  $J = 4.8, 1.5$  Hz, 1H), 7.87 (dd,  $J = 8.1, 1.5$  Hz, 1H), 7.38–7.31 (m, 2H), 7.24 (dd,  $J = 8.1, 4.6$  Hz, 1H), 6.97 (dd,  $J = 8.6, 1.1$  Hz, 1H), 6.04 (m, 1H), 4.16 (m, 2H), 3.79 (s, 3H), 3.70 (t,  $J = 5.6$  Hz, 2H), 2.61–2.51 (m, 2H). MS  $m/z$  412.2  $[M + H]^+$ .

**3-Chloro-N-[2-(dimethylamino)-4-(trifluoromethyl)phenyl]-3',6'-dihydro-(2,4'-bipyridine)-1'(2'H)-carboxamide (15).**  $^1H$  NMR (400 MHz,  $CD_3OD$ )  $\delta$  8.37 (dd,  $J = 4.8, 1.5$  Hz, 1H), 7.73 (d,  $J = 1.8$  Hz, 1H), 7.57–7.41 (m, 4H), 6.01 (m, 1H), 4.15 (m, 2H), 3.69 (t,  $J = 5.6$  Hz, 2H), 2.78–2.71 (m, 2H), 2.56–2.45 (m, 4H), 2.22 (s, 6H). MS  $m/z$  425.1  $[M + H]^+$ .

**3-Chloro-N-[3-(dimethylamino)-4-(trifluoromethyl)phenyl]-3',6'-dihydro-(2,4'-bipyridine)-1'(2'H)-carboxamide (16).**  $^1H$  NMR (400 MHz,  $CDCl_3$ )  $\delta$  8.49 (dd,  $J = 4.6, 1.5$  Hz, 1H), 7.73 (dd,  $J = 8.1, 1.3$  Hz, 1H), 7.60–7.50 (m, 2H), 7.23–7.12 (m, 2H), 6.58 (s, 1H), 6.19 (dt,  $J = 3.2, 1.7$  Hz, 1H), 4.24 (m, 2H), 3.78 (t,  $J = 5.6$  Hz, 2H), 2.96 (m, 4H), 2.80–2.68 (m, 2H), 1.00 (t,  $J = 7.1$  Hz, 6H). MS  $m/z$  453.1  $[M + H]^+$ .

**3-Chloro-5-[(dimethylamino)methyl]-N-[4-(trifluoromethyl)phenyl]-3',6'-dihydro-(2,4'-bipyridine)-1'(2'H)-carboxamide (20).**  $^1H$  NMR (400 MHz,  $DMSO-d_6$ )  $\delta$  8.95 (s, 1H), 8.42 (s, 1H), 7.82 (s, 1H), 7.73 (d,  $J = 8.0$  Hz, 2H), 7.59 (d,  $J = 8.0$  Hz, 2H), 6.23 (m, 1H), 4.20 (m, 2H), 3.70 (d,  $J = 4.0$  Hz, 2H), 3.43 (m, 2H), 2.58 (m, 2H), 2.16 (s, 6H). MS  $m/z$  439.1  $[M + H]^+$ .

**3-Chloro-5-[(2-(dimethylamino)ethyl)-N-[4-(trifluoromethyl)phenyl]-3',6'-dihydro-(2,4'-bipyridine)-1'(2'H)-carboxamide (21).**  $^1H$  NMR (400 MHz,  $CD_3OD$ )  $\delta$  8.26 (d,  $J = 1.5$  Hz, 1H), 7.73 (d,  $J = 1.8$  Hz, 1H), 7.57–7.41 (m, 4H), 6.01 (m, 1H), 4.15 (m, 2H), 3.69 (t,  $J = 5.6$  Hz, 2H), 2.78–2.71 (m, 2H), 2.56–2.45 (m, 4H), 2.22 (s, 6H). MS  $m/z$  453.1  $[M + H]^+$ .

**3-Fluoro-4-[(dimethylaminomethyl)-N-[4-(trifluoromethyl)phenyl]-3',6'-dihydro-(2,4'-bipyridine)-1'(2'H)-carboxamide (22).**  $^1H$  NMR (400 MHz,  $CD_3OD$ )  $\delta$  8.35 (d,  $J = 4.8$  Hz, 1H), 7.66–7.53 (m, 4H), 7.39 (t,  $J = 5.0$  Hz, 1H), 6.55 (s, 1H), 4.30 (m, 2H), 3.80 (t,  $J = 2.6$  Hz, 2H), 3.64 (m, 2H), 2.77 (m, 2H), 2.32 (s, 6H). MS  $m/z$  423.1  $[M + H]^+$ .

**3-Chloro-1'-[4-(trifluoromethyl)phenyl]carbonyl]-1',2'-3',6'-tetrahydro-(2,4'-bipyridine)-5-carboxylic acid (23).**  $^1H$  NMR (400 MHz,  $CD_3OD$ )  $\delta$  8.96 (d,  $J = 1.8$  Hz, 1H), 8.31 (d,  $J = 1.8$  Hz, 1H), 7.69–7.54 (m, 5H), 6.21 (s, 1H), 4.28 (m, 2H), 3.82 (t,  $J = 5.6$  Hz, 2H), 2.68 (m, 2H). MS  $m/z$  426.1  $[M + H]^+$ .

**2-[3-Chloro-1'-[4-(trifluoromethyl)phenyl]carbonyl]-1',2',3',6'-tetrahydro-(2,4'-bipyridin)-5-yl]-acetic Acid (24).**  $^1H$  NMR (400 MHz,  $DMSO-d_6$ )  $\delta$  12.71 (brs, 1H), 8.41 (d,  $J = 1.7$  Hz, 1H), 7.87 (d,

$J = 1.7$  Hz, 1H), 7.72 (d,  $J = 8.7$  Hz, 2H), 7.60 (d,  $J = 8.7$  Hz, 2H), 6.22 (m, 1H), 4.20 (m, 2H), 3.72–3.65 (m, 2H), 2.57 (m, 2H). MS  $m/z$  439.7  $[M + H]^+$ .

**3-Chloro-5-(cyanomethyl)-N-[4-(trifluoromethyl)phenyl]-3',6'-dihydro-(2,4'-bipyridine)-1'(2'H)-carboxamide (25).**  $^1H$  NMR (400 MHz,  $DMSO-d_6$ )  $\delta$  8.96 (s, 1H), 8.52 (s, 1H), 7.97 (s, 1H), 7.72 (d,  $J = 8.0$  Hz, 1H), 7.59 (d,  $J = 8.0$  Hz, 1H), 6.25 (m, 1H), 4.31 (m, 2H), 4.12 (s, 2H), 3.70 (t,  $J = 8.0$  Hz, 2H), 2.58 (m, 2H). MS  $m/z$  420.8  $[M + H]^+$ .

**3-Chloro-5-(hydroxymethyl)-N-[4-(trifluoromethyl)phenyl]-3',6'-dihydro-(2,4'-bipyridine)-1'(2'H)-carboxamide (26).**  $^1H$  NMR (400 MHz,  $CD_3OD$ )  $\delta$  8.45 (d,  $J = 2.0$  Hz, 1H), 7.96–7.85 (m, 1H), 7.74–7.49 (m, 4H), 6.15 (m, 1H), 4.67 (s, 2H), 4.27 (m, 2H), 3.81 (t,  $J = 5.6$  Hz, 2H), 2.75–2.55 (m, 2H). MS  $m/z$  412.2  $[M + H]^+$ .

**3-Chloro-5-(hydroxyethyl)-N-[4-(trifluoromethyl)phenyl]-3',6'-dihydro-(2,4'-bipyridine)-1'(2'H)-carboxamide (27).**  $^1H$  NMR (400 MHz,  $CD_3OD$ )  $\delta$  8.97 (s, 1H), 8.38 (d,  $J = 1.8$  Hz, 1H), 7.82 (d,  $J = 1.8$  Hz, 1H), 7.73 (d,  $J = 8.1$  Hz, 2H), 7.60 (d,  $J = 8.8$  Hz, 2H), 6.22–6.17 (m, 1H), 4.20 (m, 2H), 3.73–3.60 (m, 4H), 2.74 (t,  $J = 6.5$  Hz, 2H), 2.56 (m, 2H). MS  $m/z$  426.5  $[M + H]^+$ .

**3-Fluoro-4-(hydroxymethyl)-N-[4-(trifluoromethyl)phenyl]-3',6'-dihydro-(2,4'-bipyridine)-1'(2'H)-carboxamide (28).**  $^1H$  NMR (400 MHz,  $CD_3OD$ )  $\delta$  8.37 (d,  $J = 4.8$  Hz, 1H), 7.68–7.53 (m, 4H), 7.49 (t,  $J = 5.0$  Hz, 1H), 7.23 (m, 1H), 4.77 (s, 2H), 4.30 (m, 2H), 3.80 (t,  $J = 5.6$  Hz, 2H), 2.76 (m, 2H). MS  $m/z$  396.1  $[M + H]^+$ .

**3-Chloro-5-(methylsulfonamidomethyl)-N-[4-(trifluoromethyl)phenyl]-3',6'-dihydro-(2,4'-bipyridine)-1'(2'H)-carboxamide (29).**  $^1H$  NMR (400 MHz,  $DMSO-d_6$ )  $\delta$  8.98 (s, 1H), 8.49 (d,  $J = 2.0$  Hz, 1H), 7.90 (d,  $J = 1.8$  Hz, 1H), 7.78–7.64 (m, 4H), 7.60 (d,  $J = 8.8$  Hz, 3H), 6.27–6.20 (m, 1H), 4.27–4.17 (m, 6H), 3.70 (t,  $J = 5.6$  Hz, 3H), 2.96 (m, 4H), 2.58 (d,  $J = 1.5$  Hz, 3H). MS  $m/z$  489.1  $[M + H]^+$ .

**2,3-Dichloro-5-vinylpyridine (31).** Potassium-*t*-butoxide (3.14 g, 28 mmol) was added portionwise to a cooled (0 °C) slurry of methyltriphenylphosphonium bromide (10 g, 28 mol) in toluene (200 mL). The reaction mixture was stirred for 1 h and was cooled to –20 °C. After this period, a solution of **30** (4.0 g, 22.7 mmol) in tetrahydrofuran (10 mL) was added dropwise to produce a purple-colored slurry. The resulting mixture was then heated to 100 °C and stirred for additional 1 h. The reaction mixture was then cooled to room temperature, diluted with ethyl acetate (200 mL), washed with aqueous brine (150 mL), dried over  $Na_2SO_4$  and concentrated under reduced pressure to give a crude sample. The crude sample was purified by column chromatography eluting with a gradient of 0–10% ethyl acetate in hexanes to provide **31** (2.77 g, 70% yield) as a colorless oil.  $^1H$  NMR (400 MHz,  $CDCl_3$ )  $\delta$  8.30 (d,  $J = 2.2$  Hz, 1H), 7.80 (d,  $J = 2.2$  Hz, 1H), 6.63 (dd,  $J = 17.8, 11.0$  Hz, 1H), 5.86 (d,  $J = 17.8$  Hz, 1H), 5.45 (d,  $J = 11.0$  Hz, 1H). MS  $m/z$  174  $[M + H]^+$ .

**(S)-1-(5,6-Dichloropyridin-3-yl)ethane-1,2-diol (32a).** To a stirred slurry of AD-mix- $\alpha$  (8.95 g) in water (30 mL) and *t*-butanol (30 mL) at 0 °C was added a solution of **31** (0.91 g, 5.25 mmol) in *t*-butanol (5 mL). The resulting mixture was stirred at 0 °C for 2 h and at room temperature for 22 h. After this period, solid sodium sulfite (9.57 g) was added and the resulting slurry was allowed to stir for 30 min. The mixture was extracted with ethyl acetate (50 mL  $\times$  3). The organic layers were combined, washed with brine, dried over  $Na_2SO_4$  and concentrated under reduced pressure to give a crude sample. The crude sample was purified by column chromatography eluting with a gradient of 50–100% ethyl acetate in hexanes to provide **32a** (0.75 g, 70% yield) as a white solid.  $^1H$  NMR (400 MHz,  $CDCl_3$ )  $\delta$  8.29 (dd,  $J = 1.9, 0.4$  Hz, 1H), 7.87 (dd,  $J = 2.2, 0.6$  Hz, 1H), 4.87 (m, 1H), 3.84 (m, 1H), 3.66 (m, 1H), 2.83 (d,  $J = 5.9$  Hz, 1H), 2.11 (t,  $J = 5.9$  Hz, 1H). MS  $m/z$  208  $[M + H]^+$ .

**(R)-1-(5,6-Dichloropyridin-3-yl)ethane-1,2-diol (32b).** The intermediate **32b** was prepared following a similar dihydroxylation procedure as **32a** by using AD-mix- $\beta$  as oxidizing agent.  $^1H$  NMR (400 MHz,  $CDCl_3$ )  $\delta$  8.29 (dd,  $J = 1.9, 0.4$  Hz, 1H), 7.87 (dd,  $J = 2.2, 0.6$  Hz, 1H), 4.87 (m, 1H), 3.84 (m, 1H), 3.66 (m, 1H), 2.83 (d,  $J = 5.9$  Hz, 1H), 2.11 (t,  $J = 5.9$  Hz, 1H). MS  $m/z$  208  $[M + H]^+$ .

**(S)-3-Chloro-5-(1,2-dihydroxyethyl)-3',6'-dihydro-2'H-[2,4'-bipyridinyl]-1'-carboxylic Acid tert-Butyl Ester (33a).** A 50 mL round-

bottomed flask was charged with **32a** (0.70 g, 3.37 mmol), pinacol ester **6** (1.25 g, 4.04 mmol), Pd(PPh<sub>3</sub>)<sub>2</sub>Cl<sub>2</sub> (0.19 g, 0.27 mmol), potassium carbonate (0.88 g, 6.40 mmol), and a mixture of DME/EtOH/H<sub>2</sub>O (2/1/2, 20 mL). The reaction mixture was degassed and heated at 90 °C with vigorous stirring. After 2 h, the reaction mixture was cooled to room temperature and diluted with ethyl acetate (50 mL). The organic layer was washed with brine, dried over Na<sub>2</sub>SO<sub>4</sub>, and concentrated under reduced pressure. The residue was chromatographed by silica gel column chromatography eluting with a gradient of 50–100% ethyl acetate in hexanes to provide **33a** (0.96 g, 80% yield) as a colorless oil. <sup>1</sup>H NMR (400 MHz, CD<sub>3</sub>OD) δ 8.47 (s, 1H), 7.93 (s, 1H), 6.06 (m, 1H), 4.74 (t, J = 5.9 Hz, 1H), 4.12 (m, 2H), 3.67 (m, 4H), 2.54 (m, 2H), 1.52 (s, 9H). MS *m/z* 355 [M + H]<sup>+</sup>.

(*R*)-3-Chloro-5-(1,2-dihydroxyethyl)-3',6'-dihydro-2'H-[2,4']-bipyridinyl-1'-carboxylic Acid *tert*-butyl Ester (**33b**). The intermediate **33b** was prepared following a similar procedure as **33a** by using **33b** as pyridine starting material. <sup>1</sup>H NMR (400 MHz, CD<sub>3</sub>OD) δ 8.47 (s, 1H), 7.93 (s, 1H), 6.06 (m, 1H), 4.74 (t, J = 5.9 Hz, 1H), 4.12 (m, 2H), 3.67 (m, 4H), 2.54 (m, 2H), 1.52 (s, 9H). MS *m/z* 355 [M + H]<sup>+</sup>.

(*S*)-1-(3-Chloro-1',2',3',6'-tetrahydro-[2,4']bipyridinyl-5-yl)-ethane-1,2-diol (**34a**). To a solution of **33a** (0.90 g, 2.54 mmol) in CH<sub>2</sub>Cl<sub>2</sub> (10 mL) at 0 °C was added 4 M HCl in Et<sub>2</sub>O (10 mL). The ice bath was removed, and the resulting mixture was stirred at 40 °C for 20 h. After this period, the reaction mixture was allowed to cool to room temperature and the resulting solid was filtered, washed with Et<sub>2</sub>O (20 mL), and dried under reduced pressure to provide **34a** as an HCl salt (0.70 g, 95% yield). <sup>1</sup>H NMR (400 MHz, CD<sub>3</sub>OD) δ 8.74 (s, 1H), 8.52 (s, 1H), 6.38 (m, 1H), 4.91 (m, 1H), 4.00 (m, 2H), 3.75 (m, 4H), 3.54 (t, J = 5.9 Hz, 2H), 2.89 (m, 2H). MS *m/z* 255 [M + H]<sup>+</sup>.

(*R*)-1-(3-Chloro-1',2',3',6'-tetrahydro-[2,4']bipyridinyl-5-yl)-ethane-1,2-diol (**34b**). <sup>1</sup>H NMR (400 MHz, CD<sub>3</sub>OD) δ 8.74 (s, 1H), 8.52 (s, 1H), 6.38 (m, 1H), 4.91 (m, 1H), 4.00 (m, 2H), 3.75 (m, 4H), 3.54 (t, J = 5.9 Hz, 2H), 2.89 (m, 2H). MS *m/z* 255 [M + H]<sup>+</sup>.

(*S*)-3-Chloro-5-(1,2-dihydroxyethyl)-*N*-[4-(trifluoromethyl)phenyl]-3',6'-dihydro-(2,4'-bipyridine)-1'(2'H)-carboxamide (**35**). General procedure for syntheses of **35** and **36**. To a suspension of **34a** (800 mg, 2.45 mmol) in anhydrous CH<sub>2</sub>Cl<sub>2</sub> (20 mL) at 0 °C was added diisopropylethylamine (DIEA, 2 mL) and 1-isocyanato-4-(trifluoromethyl)benzene (462 mg, 2.45 mmol). The reaction mixture was warmed to room temperature and further stirred for 2 h. After concentrated under reduced pressure, the residue was chromatographed by silica gel chromatography column eluting with a gradient of 0–20% MeOH in CH<sub>2</sub>Cl<sub>2</sub> to provide **35** (0.60 g, 56% yield) as a white solid. <sup>1</sup>H NMR (400 MHz, CD<sub>3</sub>OD) δ 8.49 (d, J = 1.5 Hz, 1H), 7.94 (dd, J = 1.3 Hz, 1H), 7.71–7.51 (m, 4H), 6.14 (m, 1H), 4.78 (t, J = 5.6 Hz, 1H), 4.35–4.23 (m, 2H), 3.82 (t, J = 5.6 Hz, 2H), 3.73–3.64 (m, 2H), 2.65 (m, 2H). MS *m/z* 442.1 [M + H]<sup>+</sup>.

(*R*)-3-Chloro-5-(1,2-dihydroxyethyl)-*N*-[4-(trifluoromethyl)phenyl]-3',6'-dihydro-(2,4'-bipyridine)-1'(2'H)-carboxamide (**36**). <sup>1</sup>H NMR (400 MHz, CD<sub>3</sub>OD) δ 8.49 (d, J = 1.5 Hz, 1H), 7.94 (dd, J = 1.3 Hz, 1H), 7.71–7.51 (m, 4H), 6.14 (m, 1H), 4.78 (t, J = 5.6 Hz, 1H), 4.35–4.23 (m, 2H), 3.82 (t, J = 5.6 Hz, 2H), 3.73–3.64 (m, 2H), 2.65 (m, 2H). MS *m/z* 442.1 [M + H]<sup>+</sup>.

(*S*)-4-[3-Chloro-5-(1,2-dihydroxyethyl)pyridin-2-yl]-*N*-[5-(trifluoromethyl)pyridin-2-yl]-3',6'-dihydropyridine-1'(2'H)-carboxamide (**37**). General procedure for syntheses of **37**–**39**. To a stirred solution of 2-amino-5-(trifluoromethyl)pyridine (12.1 g, 74.1 mmol) at 0 °C in CH<sub>2</sub>Cl<sub>2</sub> (50 mL) was added phenylchloroformate (12.7 g, 81.5 mmol). Then pyridine (6.3 mL, 81.5 mmol) was added dropwise. The reaction mixture was stirred for 2 h at 0 °C. The resulting solid was filtered off and washed with CH<sub>2</sub>Cl<sub>2</sub> to afford phenyl(5-(trifluoromethyl)pyridin-2-yl)carbamate (16.7 g). In a separate flask, to a suspension of **34a** as its HCl salt (9.36 g, 32.27 mmol) in anhydrous CH<sub>2</sub>Cl<sub>2</sub> (50 mL) at –20 °C was added phenyl(5-(trifluoromethyl)pyridin-2-yl)carbamate (9.10 g, 32.27 mmol) in one portion. Then diisopropylethylamine (DIEA 14 mL, 80.65 mmol) was added dropwise to the mixture over 20 min. The resulting reaction mixture was stirred for 2 h at –20 °C. After this period, the reaction mixture was concentrated under reduced pressure to give a crude

sample that was purified by silica gel column chromatography eluting with a gradient of 0–20% MeOH in CH<sub>2</sub>Cl<sub>2</sub> to provide **37** (10.51 g, 74% yield) as a white solid. <sup>1</sup>H NMR (500 MHz, DMSO-*d*<sub>6</sub>) δ 9.84 (s, 1H), 8.63 (dd, J = 2.4, 1.0 Hz, 1H), 8.48 (d, J = 1.8 Hz, 1H), 8.13–8.04 (m, 1H), 8.03–7.97 (m, 1H), 7.84 (d, J = 1.8 Hz, 1H), 6.19 (m, 1H), 5.55 (d, J = 4.8 Hz, 1H), 4.86 (t, J = 5.8 Hz, 1H), 4.62 (q, J = 5.6 Hz, 1H), 4.22 (d, J = 2.8 Hz, 2H), 3.72 (t, J = 5.6 Hz, 2H), 3.56 (m, 1H), 3.51–3.43 (m, 1H), 2.58 (m, 2H). MS *m/z* 443.1 [M + H]<sup>+</sup>. Anal. Calcd for C<sub>19</sub>H<sub>18</sub>ClF<sub>3</sub>N<sub>4</sub>O<sub>3</sub>: C 51.53; H 4.10; N 12.65. Found: C 51.58; H 3.83; N 12.71.

(*S*)-4-[3-Chloro-5-(1,2-dihydroxyethyl)pyridin-2-yl]-*N*-[6-(trifluoromethyl)pyridin-3-yl]-3',6'-dihydropyridine-1'(2'H)-carboxamide (**38**). The analogue **38** was prepared following a similar procedure as **37** by coupling intermediate **34a** with phenyl(6-(trifluoromethyl)pyridin-2-yl)carbamate. <sup>1</sup>H NMR (400 MHz, CD<sub>3</sub>OD) δ 8.69 (d, J = 2.4 Hz, 1H), 8.37 (d, J = 1.5 Hz, 1H), 8.06 (dd, J = 8.6, 2.2 Hz, 1H), 7.83 (d, J = 1.5 Hz, 1H), 7.62 (d, J = 8.8 Hz, 1H), 6.03 (m, 1H), 4.66 (t, J = 5.7 Hz, 1H), 4.18 (m, 2H), 3.71 (t, J = 5.6 Hz, 2H), 3.63–3.53 (m, 2H), 2.58–2.52 (m, 2H). MS *m/z* 443.1 [M + H]<sup>+</sup>.

(*R*)-4-[3-Chloro-5-(1,2-dihydroxyethyl)pyridin-2-yl]-*N*-[5-(trifluoromethyl)pyridin-2-yl]-3',6'-dihydropyridine-1'(2'H)-carboxamide (**39**). <sup>1</sup>H NMR (500 MHz, DMSO-*d*<sub>6</sub>) δ 9.84 (s, 1H), 8.63 (dd, J = 2.4, 1.0 Hz, 1H), 8.48 (d, J = 1.8 Hz, 1H), 8.13–8.04 (m, 1H), 8.03–7.97 (m, 1H), 7.84 (d, J = 1.8 Hz, 1H), 6.19 (m, 1H), 5.55 (d, J = 4.8 Hz, 1H), 4.86 (t, J = 5.8 Hz, 1H), 4.62 (q, J = 5.6 Hz, 1H), 4.22 (d, J = 2.8 Hz, 2H), 3.72 (t, J = 5.6 Hz, 2H), 3.56 (m, 1H), 3.51–3.43 (m, 1H), 2.58 (m, 2H). MS *m/z* 443.1 [M + H]<sup>+</sup>.

## ■ ASSOCIATED CONTENT

### ☎ Supporting Information

Pharmacological selectivity profile of compound **37**, effect of compound **37** on body temperature after repeated administration to naïve and CFA treated rats, results of PK/PD relationship study for compound **37**. This material is available free of charge via the Internet at <http://pubs.acs.org>.

## ■ AUTHOR INFORMATION

### ✉ Corresponding Author

\*Phone: 1-202-905-6936. E-mail: [laykea@chemist.com](mailto:laykea@chemist.com).

### Notes

The authors declare no competing financial interest.

## ■ ACKNOWLEDGMENTS

We thank members of the Purdue–Shionogi research collaboration for the support of this program.

## ■ ABBREVIATIONS USED

TRPV1, transient receptor potential vanilloid 1; SAR, structure–activity relationship; BCTC, 4-(3-chloro-2-pyridinyl)-*N*-[4-(1,1-dimethylethyl)phenyl]-1-piperazinecarboxamide; CAP, capsaicin; CHO cell, Chinese hamster ovary cell; FLIPR, fluorometric imaging plate reader; CFA, complete Freund's adjuvant; EP, electrophysiology

## ■ REFERENCES

- (1) Szallasi, A.; Blumberg, P. M. Vanilloid (capsaicin) receptors and mechanisms. *Pharmacol. Rev.* **1999**, *51*, 159–211.
- (2) Caterina, M. J.; Schumacher, M. A.; Tominaga, M.; Rosen, T. A.; Levine, J. D.; Julius, J. D. The capsaicin receptor: a heat-activated ion channel in the pain pathway. *Nature* **1997**, *389*, 816–824.
- (3) Brederson, J. D.; Kym, P. R.; Szallasi, A. Targeting TRP channels for pain relief. *Eur. J. Pharmacol.* **2013**, *716*, 61–67.
- (4) Gunthrope, M. J.; Chizh, B. A. Clinical development of TRPV1 antagonists: targeting a pivotal point in the pain pathway. *Drug Discovery Today* **2009**, *14*, 56–67.

- (5) Holzer, P. The pharmacological challenge to tame the transient receptor potential vanilloid-1 (TRPV1) nociceptor. *Br. J. Pharmacol.* **2008**, *155*, 1145–1162.
- (6) Caterina, M. J.; Leffler, A.; Malmberg, A. B.; Martin, W. J.; Trafton, J.; Petersen-Zeitz, K. R.; Koltzenburg, M.; Basbaum, A. I.; Julius, D. Impaired nociception and pain sensation in mice lacking the capsaicin receptor. *Science* **2000**, *288*, 306–313.
- (7) Davis, J. B.; Gray, J.; Gunthrope, M. J.; Hatcher, J. P.; Davey, P. T.; Overend, P.; Harries, M. H.; Latcham, J.; Clapham, C.; Atkinson, K.; Hughes, S. A.; Rance, K.; Grau, E.; Harper, A. J.; Pugh, P. L.; Rogers, D. C.; Bingham, S.; Randall, A.; Sheardown, S. A. Vanilloid receptor-1 is essential for inflammatory thermal hyperalgesia. *Nature* **2000**, *405*, 183–187.
- (8) Chizh, B. A.; O'Donnell, M. B.; Napolitano, A.; Wang, J.; Brooke, A. C.; Aylott, M. C.; Bullman, J. N.; Gray, E. J.; Lai, R. Y.; Williams, P. M.; Appleby, J. M. The effects of the TRPV1 antagonist SB-705498 on TRPV1 receptor-mediated activity and inflammatory hyperalgesia in humans. *Pain* **2007**, *132*, 132–141.
- (9) Gavva, N. R.; Treanor, J. J.; Garami, A.; Fang, L.; Surapaneni, S.; Akrami, A.; Alvarez, F.; Bak, A.; Darling, M.; Gore, A.; Jang, G. R.; Kesslak, J. P.; Ni, L.; Norman, M. H.; Palluconi, G.; Rose, M. J.; Salfi, M.; Tan, E.; Romanovsky, A. A.; Banfield, C.; Davar, G. Pharmacological blockade of the vanilloid receptor TRPV1 elicits marked hyperthermia in humans. *Pain* **2008**, *136*, 202–210.
- (10) Rowbotham, M. C.; Nothaft, W.; Duan, W. R.; Wang, Y.; Faltynek, C.; McGaraughty, S.; Chu, K. L.; Svensson, P. Oral and cutaneous thermosensory profile of selective TRPV1 inhibition by ABT-102 in a randomized healthy volunteer trial. *Pain* **2011**, *152*, 1192–1200.
- (11) Schaffler, K.; Reeh, P.; Duan, W. R.; Best, A. E.; Othman, A. A.; Faltynek, C. R.; Locke, C.; Nothaft, W. An oral TRPV1 antagonist attenuates laser radiant-heat-evoked potentials and pain ratings from UV(B)-inflamed and normal skin. *Br. J. Clin. Pharmacol.* **2013**, *75*, 404–414.
- (12) (a) Kyle, D. J.; Tafesse, L. TRPV1 antagonists: a survey of recent patent literature. *Expert Opin. Ther. Pat.* **2006**, *16*, 977–996. (b) Voight, E. A.; Kort, M. E. Transient receptor potential vanilloid-1 antagonists: a survey of recent patent literature. *Expert Opin. Ther. Pat.* **2010**, *20*, 1107–1122.
- (13) (a) Tafesse, L.; Sun, Q.; Schmid, L. A.; Valenzano, K. J.; Rotshteyn, Y.; Su, S.; Kyle, D. J. Synthesis and evaluation of pyridazinylpiperazines as vanilloid receptor 1 antagonists. *Bioorg. Med. Chem. Lett.* **2004**, *14*, 5513–5519. (b) Sun, Q.; Tafesse, L.; Islam, K.; Zhou, X.; Victory, S. F.; Zhang, C.; Hachicha, M.; Schmid, L. A.; Patel, A.; Rotshteyn, Y.; Valenzano, K. J.; Kyle, D. J. 4-(2-Pyridyl)piperazine-1-carboxamides: potent vanilloid receptor 1 antagonists. *Bioorg. Med. Chem. Lett.* **2003**, *13*, 3611–3616.
- (14) Swanson, D. M.; Dubin, A. E.; Shah, C.; Nasser, N.; Chang, L.; Dax, S. L.; Jetter, M.; Breitenbacher, J. G.; Liu, C.; Mazur, C.; Lord, B.; Donzales, L.; Hoey, K.; Rizzolio, M.; Bogenstaetter, M.; Codd, E. E.; Lee, D. H.; Zhang, S.-P.; Chaplan, S. R.; Carruthers, N. I. Identification and biological evaluation of 4-(3-trifluoromethylpyridin-2-yl)piperazine-1-carboxylic acid (5-trifluoromethylpyridin-2-yl)amide, a high affinity TRPV1 (VR1) vanilloid receptor antagonist. *J. Med. Chem.* **2005**, *48*, 1857–1872.
- (15) Ognyanov, V. I.; Balm, C.; Bannon, A. W.; Bo, Y.; Dominguez, C.; Fotsch, C.; Gore, V. K.; Klionsky, L.; Ma, V. V.; Qian, Y.-X.; Tamir, R.; Wang, X.; Xi, N.; Xu, S.; Zhu, D.; Gavva, N. R.; Treanor, J. J. S.; Norman, M. H. Design of potent, orally available antagonists of the transient receptor potential vanilloid 1. A structure–activity relationships of 2-piperazin-1-yl-1H-benzimidazoles. *J. Med. Chem.* **2006**, *49*, 3719–3742.
- (16) Valenzano, K. J.; Grant, E. R.; Wu, G.; Hachicha, M.; Schmid, L.; Tafesse, L.; Sun, Q.; Rotshteyn, Y.; Francis, J.; Limberis, J.; Malik, S.; Whittemore, E. R.; Hodges, D. N-(4-Tertiarybutylphenyl)-4-(3-chloropyridin-2-yl)tetrahydropyrazine-1(2H)-carboxamide (BCTC), a novel, orally effective vanilloid receptor 1 antagonist with analgesic properties. I. In vitro characterization and pharmacokinetic properties. *J. Pharmacol. Exp. Ther.* **2003**, *306*, 377–38.
- (17) Kym, P. R.; Kort, M. E.; Hutchins, C. W. Analgesic potential of TRPV1 antagonists. *Biochem. Pharmacol.* **2009**, *78*, 211–216.
- (18) Suh, Y. G.; Oh, U. Activation and activators of TRPV1 and their pharmaceutical implication. *Curr. Pharm. Des.* **2005**, *11*, 474–484.
- (19) Garami, A.; Shimansky, Y. P.; Pakai, E.; Oliveira, D. L.; Gavva, N. R.; Romanovsky, A. A. Contributions of different modes of TRPV1 activation to TRPV1 antagonist-induced hyperthermia. *J. Neurosci.* **2010**, *30*, 1435–1440.
- (20) Lehto, S. G.; Tamir, R.; Deng, H.; Klionsky, L.; Kunag, R.; Le, A.; Lee, D.; Louis, J.-C.; Magal, E.; Manning, B. H.; Rubino, J.; Surapaneni, S.; Tamayo, N.; Wang, T.; Wang, J.; Wang, W.; Youngblood, B.; Zhang, M.; Zhu, D.; Norman, M. H.; Gavva, N. R. Antihyperalgesic effects of (R,E)-N-(2-hydroxy-2,3-dihydro-1H-inden-4-yl)-3-(2-piperidin-1-yl)-4-(trifluoromethylphenyl)-acrylamide (AMG8562), a novel transient receptor potential vanilloid type 1 modulator that does not cause hyperthermia in rats. *J. Pharmacol. Exp. Ther.* **2008**, *326*, 218–229.
- (21) (a) Walker, K. M.; Urban, L.; Medhurst, S. J.; Patel, S.; Panesar, M.; Fox, A. J.; McIntyre, P. The VR1 antagonist capsazepine reverses mechanical hyperalgesia in models of inflammatory and neuropathic pain. *J. Pharmacol. Exp. Ther.* **2003**, *304*, 56–62. (b) Pomonis, J. D.; Harrison, J. E.; Mark, L.; Bristol, D. R.; Valenzano, K. J.; Walker, K. N-(4-Tertiarybutylphenyl)-4-(3-chloropyridin-2-yl)tetrahydropyrazine-1(2H)-carboxamide (BCTC), a novel, orally effective vanilloid receptor 1 antagonist with analgesic properties. II. In vivo characterization in rat models of inflammatory and neuropathic pain. *J. Pharmacol. Exp. Ther.* **2003**, *306*, 387–393.
- (22) Reilly, R. M.; McDonald, H. A.; Puttarcken, P. S.; Joshi, S. K.; Lewis, L.; Pai, M.; Franklin, P. H.; Segreti, J. A.; Needlands, T. R.; Han, P.; Chen, J.; Mantyh, P. W.; Ghilardi, J. R.; Turner, T. M.; Voight, E. A.; Daanen, J. F.; Schmidt, R. G.; Gomtsyan, A.; Kort, M. E.; Faltynek, C. R.; Kym, P. R. Pharmacology of modality-specific transient receptor potential vanilloid-1 antagonists that do not alter body temperature. *J. Pharmacol. Exp. Ther.* **2012**, *342*, 416–428.
- (23) Pitcher, T. E.; Nicholson, J. R.; Neuman, R.; Machin, I. Different interpretation of the hot plate test in rats. *Proceedings of Measuring Behavior, Eindhoven, The Netherlands, August 24–27, 2010*; Spink, A. J., Grieco, F., Krips, O. E., Loijens, L. W. S., Noldus, L. P. J., Zimmerman, P. H., Eds.; Noldus Information Technology: The Netherlands, 2010; p 426.
- (24) Gunthorpe, M. J.; Hannan, S. L.; Smart, D.; Jerman, J. C.; Arpino, S.; Smith, G. D.; Brough, S.; Wright, J.; Egerton, J.; Lappin, S. C.; Holland, V. A.; Winborn, K.; Thompson, M.; Rami, H. K.; Randall, A.; Davis, J. B. Characterization of SB-705498, a potent and selective vanilloid receptor-1 (VR1/TRPV1) antagonist that inhibits the capsaicin-, acid-, and heat-mediated activation of the receptor. *J. Pharmacol. Exp. Ther.* **2007**, *321*, 1183–1192.
- (25) Gavva, N. R.; Tamir, R.; Qu, Y.; Klionsky, L.; Zhang, T. J.; Immke, D.; Wang, J.; Zhu, D.; Vanderah, T. W.; Porreca, F.; Doherty, E. M.; Norman, M. H.; Wild, K. D.; Bannon, A. W.; Louis, J.-C.; Treanor, J. J. S. AMG 9810 [(E)-3-(4-t-Butylphenyl)-N-(2,3-dihydrobenzo[b][1,4]dioxin-6-yl)acrylamide], a novel vanilloid receptor 1 (TRPV1) antagonist with antihyperalgesic properties. *J. Pharmacol. Exp. Ther.* **2005**, *313*, 474–484.